

# Spatial Pricing in Ride-Sourcing Markets under a Congestion Charge

Sen Li<sup>a</sup>, Hai Yang<sup>a</sup>, Kameshwar Poolla<sup>b</sup>, Pravin Varaiya<sup>b</sup>

<sup>a</sup>*Department of Civil and Environmental Engineering, Hong Kong University of Science and Technology*

<sup>b</sup>*Department of Electrical Engineering and Computer Science, University of California, Berkeley*

---

## Abstract

This paper studies the optimal spatial pricing for a ride-sourcing platform subject to a congestion charge. The platform determines the ride prices over the transportation network to maximize its profit, while the regulatory agency imposes the congestion charge to reduce traffic congestion in the urban core. A network economic equilibrium model is proposed to capture the intimate interactions among passenger demand, driver supply, passenger and driver waiting times, platform pricing, vehicle repositioning and flow balance over the transportation network. The overall optimal pricing problem is cast as a non-convex program. An algorithm is proposed to approximately compute its optimal solution, and a tight upper bound is established to evaluate its performance loss with respect to the globally optimal solution. Using the proposed model, we compare the impacts of three forms of congestion charge: (a) a one-directional cordon charge on ride-sourcing vehicles that enter the congestion area; (b) a bi-directional cordon charge on ride-sourcing vehicles that enter or exit the congestion area; (c) a trip-based congestion charge on all ride-sourcing trips. We show that the one-directional congestion charge not only reduces the ride-sourcing traffic in the congestion area, but also reduces the travel cost outside the congestion zone and benefits passengers in these underserved areas. We establish that in all congestion charge schemes the largest share of the tax burden is carried by the platforms, as opposed to passengers and drivers. We further show that compared to other congestion charges, the one-directional cordon charge is more effective in congestion mitigation: to achieve the same congestion-mitigation target, it imposes a smaller cost on passengers, drivers, and the platform. On the other hand, compared with the other charges, the trip-based congestion charge is more effective in revenue-raising: to raise the same tax revenue, it leads to a smaller loss to passengers, drivers, and the platform. We validate these results through realistic numerical studies for San Francisco.

*Keywords:* ride-sourcing, cordon price, spatial pricing, network model

---

## Nomenclature

- $\alpha$  Trade-off between money and waiting time for ride-sourcing passengers
- $\beta$  Trade-off between money and in-vehicle travel time for ride-sourcing passengers
- $\epsilon$  Parameter of the passenger demand logit model
- $\sigma$  Parameter of the driver supply logit model
- $\eta$  Parameter of the driver repositioning logit model

---

*Email addresses:* cesli@ust.hk (Sen Li), cehyang@ust.hk (Hai Yang), poolla@berkeley.edu (Kameshwar Poolla), varaiya@berkeley.edu (Pravin Varaiya)

$\lambda_{ij}$	Arrival rate (per minute) of ride-sourcing passengers traveling from zone $i$ to zone $j$
$\lambda_{ij}^0$	Arrival rate (per minute) of potential passengers traveling from zone $i$ to zone $j$
$\lambda_{11}$	Arrival rate (per minute) of passengers traveling from $\mathcal{C}$ to $\mathcal{C}$
$\lambda_{12}$	Arrival rate (per minute) of passengers traveling from $\mathcal{C}$ to $\mathcal{R}$
$\lambda_{21}$	Arrival rate (per minute) of passengers traveling from $\mathcal{R}$ to $\mathcal{C}$
$\lambda_{22}$	Arrival rate (per minute) of passengers traveling from $\mathcal{R}$ to $\mathcal{R}$
$\mathbb{P}_{ij}$	Probability of vehicle repositioning from zone $i$ to zone $j$ before congestion charge
$\tilde{\mathbb{P}}_{ij}$	Probability of vehicle repositioning from zone $i$ to zone $j$ after congestion charge
$\sigma_i$	Probability of getting matched to a passenger while a driver traverses zone $i$
$\mathcal{C}$	Set of indexes of the congested zones
$\mathcal{R}$	Set of indexes of the remote zones
$\mathcal{S}$	Set of indexes of the southwest corner of San Francisco
$\mathcal{V}$	Set of indexes of all the $M$ zones
$c_{ij}$	Generalized travel cost (\$) of ride-sourcing passengers from zone $i$ to zone $j$
$d_{ij}^{\mathcal{C}}$	Average trip distance (mile) from zone $i$ to zone $j$ within the congestion area $\mathcal{C}$
$d_{ij}^{\mathcal{R}}$	Average trip distance (mile) from zone $i$ to zone $j$ within the remote area $\mathcal{R}$
$d_{ij}$	Average trip distance (mile) from zone $i$ to zone $j$
$f_{ij}$	Intended driver repositioning flow (per minute) from zone $i$ to zone $j$
$\tilde{f}_{ij}$	Actual driver repositioning flow (per minute) from zone $i$ to zone $j$
$L$	Parameter of the pickup time model
$M$	Number of zones in the city
$N$	Vehicle hours supplied by the ride-sourcing drivers
$N_0$	Potential vehicle hours supplied by the drivers
$N_i^I$	Average number of idle drivers (idle vehicle hours) in zone $i$
$N_{\mathcal{C}}$	Total number of ride-sourcing vehicles in the congestion area.
$N_{\mathcal{R}}$	Total number of ride-sourcing vehicles in the remote area.
$N_{\mathcal{S}}$	Total number of ride-sourcing vehicles in the southwest corner of San Francisco.
$q$	Average driver wage per unit time
$r_i$	Ride fare (\$/min) for ride-sourcing trips starting from zone $i$
$t_{ij}$	Travel time (minute) from zone $i$ to zone $j$
$w_i^p$	Average waiting time (minute) for passengers starting from zone $i$

- $w_i^d$  Average waiting time (minute) for drivers in zone  $i$  to pick up the next passenger
- $v_c$  Average speed (mph) in the congestion area.
- $v_r$  Average speed (mph) in the remote area.

## 1. Introduction

Ride-sourcing platforms like Uber, Lyft and Didi, have greatly changed the way many people commute in the city. They offer on-demand mobility services to hundreds of millions of passengers from anywhere at anytime. They generate substantial travel demand that would not have existed. They replace many trips that otherwise would have been taken by public transit, taxis and walking. They also raise public concerns about congestion, emissions, and social equity.

As ride-sourcing platforms keep disrupting urban transportation, some city governments have responded by imposing various congestion-mitigation policies. In Feb 2019, New York City (NYC) passed a Tax Law imposing a \$2.75/trip congestion surcharge on all ride-sourcing trips that begin in, end in, or pass through the congestion area of NYC in Manhattan, south of and excluding 96th Street [1]. In Apr 2019, the New York State Assembly passed the Traffic Mobility Act (Bill No. 09633) authorizing the Metropolitan Transportation Authority (MTA) to charge a cordon price between \$10 and \$15 on vehicles entering south of 61st Street in Manhattan by 2021 [2]. It is expected that this cordon price will raise \$3.5B/year for MTA to upgrade its aging transit infrastructure. In Jan 2020, the City of Chicago introduced a tiered congestion surcharge on ride-sourcing trips [3]: a \$3/trip charge on solo rides that start or end in the designated downtown area, a \$1.25/trip charge on other solo rides, and a \$0.65/trip charge on other shared rides. The revenue collected from this tax will be used to subsidize public transit and cab drivers. In addition to NYC and Chicago, San Francisco imposed a Traffic Congestion Mitigation excise tax of 1.5% to 3.25% (effective January 1, 2020) on fares for rides originating in San Francisco that are facilitated by commercial ride-share companies or are provided by an autonomous vehicle or private transit services vehicle [4]. Massachusetts [5] is proposing similar congestion-mitigating measures for legislative approval. Bottom line: the regulatory landscape is changing.

Despite congestion-limiting regulations that target ride-sourcing traffic, there is still a debate whether ride-sourcing platforms actually contribute to increased traffic congestion. On the one hand, various studies have demonstrated the positive correlation between ride-sourcing platforms and traffic congestion. For instance, the San Francisco County Transportation Authority [6] estimated that ride-sourcing platforms contributed 50% of the increase in traffic congestion in San Francisco between 2010 and 2016. Schaller [7] reported that the number of ride-sourcing vehicles increased by 59% in NYC between 2013 and 2017, while average traffic speed declined by 15% and vehicle miles traveled (VMT) increased by 36%. A recent study [8] collected ride-sourcing data in NYC and concluded that the growth of ride-sourcing platforms is the major contributing factor making urban traffic congestion worse. On the other hand, another study concluded that ride-sourcing vehicles do not account for a significant portion of the overall traffic. Fehr & Peers examined the combined VMT by Uber and Lyft in six metropolitan cities in the US [9]. They showed that the VMT of Uber and Lyft is vastly outstripped by personal and commercial vehicles, accounting only for 13.4 percent of VMT in San Francisco County, 8 percent in Boston and 7.2 percent in Washington, DC. However, we emphasize that a city’s traffic congestion exhibits a strong spatial and temporal pattern, with most of the congestion concentrated in a small area of the city for short periods of time. Moreover, the spatial and temporal pattern of the city’s traffic is highly correlated with the demand and supply pattern of the ride-sourcing market. Therefore using average VMT throughout the city as the indicator of congestion will lead to a significant underestimate of the congestion caused by ride-sourcing vehicles. Hence the spatial and temporal aspects are crucial in estimating and addressing these congestion externalities.

This paper focuses on the spatial aspect of the ride-sourcing market and proposes a model to predict the impact of congestion charges on ride-sourcing services over a transportation network. An economic equilibrium model is formulated to capture the opposing incentives of passengers, drivers, and the platform. The model is built upon a traffic network to characterize the spatial distribution of passengers and drivers in the ride-sourcing market. By incorporating the spatial aspect in the economic model, our framework can capture the intimate interactions among passenger spatial distribution, driver spatial distribution, passenger waiting time, driver waiting time, idle driver repositioning, traffic congestion, network flow balance and location-differentiated pricing. The major contributions of this paper are summarized below:

- We develop a networked market equilibrium model that simultaneously captures the essential factors in a ride-sourcing network, including passenger waiting time, driver waiting time, passenger spatial distribution, driver spatial distribution, driver repositioning strategies, traffic congestion, network flow balance and platform pricing.
- We cast the optimal spatial pricing problem as a non-convex program and propose an efficient algorithm to approximately compute its optimal solutions. A tight upper bound is established to evaluate the performance of the proposed algorithm.
- We evaluate the impact of three forms of congestion charge: (a) a one-directional cordon price that penalizes all vehicles (including idle ones) entering the congestion area, (b) a bi-directional cordon price that penalizes all vehicles (including idle ones) for entering or exiting the congestion area, and (c) a trip-based congestion charge on all ride-sourcing trips.<sup>1</sup> We show that the one-directional congestion charge not only reduces ride-sourcing traffic in the congestion area, but also reduces the travel cost outside of the congestion area and benefits passengers in these underserved zones. We verify that for all three congestion charges the highest share of the tax burden is borne by the platform as opposed to passengers and drivers. We also show that compared with other congestion charges, the one-directional cordon price is most effective in congestion-mitigation, while the trip-based congestion charge is most effective in revenue-raising: to achieve the same traffic mitigating target (or revenue-raising target), the one-directional charge (or trip-based congestion charge) imposes a smaller cost on passengers, drivers and the platform.
- The proposed framework is validated through realistic simulations based on synthetic ride-sourcing data for San Francisco. Through sensitivity analysis, we show that the results and insights derived from our model are robust with respect to the variation of model parameters.

## 2. Related work

A growing literature addresses the supply-demand equilibrium of mobility services over a transportation network. In a pioneering work [10], a network model was developed to describe the movement of idle and occupied taxi vehicles on the road network to look for passengers and provide transportation services. It offers interesting insights on the interactions among the number of taxis, the average taxi utilization and the passenger waiting time. This model was later extended to incorporate various other features, such as traffic congestion and demand elasticity [11], competition and regulation [12], bilateral taxi-customer searching and meeting [13], and multiple user classes and vehicle modes [14]. While these works primarily focus on street-hailing of taxi services, they were later adapted to the study of e-hailing services. For instance, [15] considered a traffic network model with (e-hailing) ride-sourcing services, which captured both intra-zone matching and inter-zone matching to account for cruising and deadheading vacant trips at the same

---

<sup>1</sup>The trip-based congestion charge is imposed on a per-trip basis, and exempts idle vehicles cruising for passengers.

time. By numerical studies, they showed that neglecting inter-zone matching may lead to significant bias in evaluating the vacancy/empty miles generated by the ride-sourcing platforms. [16] developed a general economic equilibrium model to describe the equilibrium state of a transportation system with solo drivers and the ride-sourcing platform, which provides insights to understand the relationship between ride-sourcing service, deadhead miles, and its impact on congestion. [17] proposed a theoretical model to identify the spatial distortion of supply from demand, and showed that a smaller platform tends to distort the supply of drivers towards more densely populated areas due to network effects.

However, all of the aforementioned works primarily focus on equilibrium analysis for a given price, so the price-formation mechanism is missing. In practice, ride-sourcing platforms use pricing as a powerful tool to balance supply and demand for more efficient matching, which defines the fundamental difference between the emerging ride-sourcing service and traditional taxi service. This has been widely studied in the network setting as the optimal spatial pricing problem, where the platform determines the location-differentiated prices to maximize its profit and passengers and drivers respond to these prices by making mode choices or repositioning decisions. For instance, [18] studied spatial price discrimination in a ride-sharing platforms that serves a networks of locations, and showed that platform profit and consumer surplus at the equilibrium are maximized when the demand pattern is balanced across the transportation network. [19] developed a discrete-time geometric matching framework over the transportation network to explore the effects of spatial pricing on the ride-sourcing market, and showed that the platform may increase the ride price to avoid inefficient supply if spatial price differentiation is not allowed. [20] built a bi-level model to capture the decision-making of both platforms and ride-sourcing customers and revealed that the platform profit at a particular zone can be influenced by ride requests from other zones. [21] considered surge pricing in a ride-sourcing market with independent drivers that strategically move between zones and showed that surge price can be useful even in zones where supply exceeds demand. [22] proposed a spatial-temporal pricing mechanism for a multi-period, multi-location model and showed that the mechanism is incentive-aligned, individually rational, budget balanced, and welfare-optimal. [23] studied the optimal spatial pricing problem with a Stackelberg framework considering the ride-sourcing platform’s congestion externality. [24] studies the impact of the ride-sourcing platform on the taxi system by developing a spatial equilibrium model that not only balances the demand and supply of the taxi market but also captures the possible adoption of emerging e-hailing apps by the taxi drivers. [25] considered a fleet of electrified vehicles providing electricity services and mobility services at the same time, and demonstrated its synergetic value in reducing the transportation spatial imbalance. *We emphasize that our paper differs from these works in that we simultaneously capture locational differentiated prices, passenger waiting time, driver waiting time, idle driver repositioning, traffic congestion, and network flow balance. These crucial elements are combined in a spatial pricing model to investigate the impact of congestion charges on the ride-sourcing networks.*

Road pricing has been a research topic for decades. The idea was initially proposed in [26], which subsequently inspired several important works including [27], [28], and [29]. Various pricing schemes were explored [30], [31] following these seminal works. For instance, in [32] the congested assignment network model was used to test four road pricing systems, with charges based on cordon crossed, distance traveled, time spent in traveling and time spent in congestion. They showed that when rerouting effects are considered, the benefit of road pricing is significantly smaller than expected. [33] considered the joint optimization of toll levels and toll locations on a road network using a mathematical program with mixed variables. [34] proposed a convergent trial-and-error implementation method for a form of road pricing congestion control under the condition that both the link travel time and the travel demand are unknown. [35] considered the dynamic road pricing problem by modeling departure time decision and mode and route choices as endogenous variables. Various link-tolling schemes are analyzed using a dynamic network simulator. [36] determined a Pareto-improving pricing scheme for relieving traffic congestion in a multimodal transportation network that maximizes social benefit without increasing the travel expenses of the stakeholders. [37] explored the effect of income on traveler choice and proposed a theoretical model to design efficient and equitable road pricing schemes. More recently, road pricing has been investigated for autonomous vehicles

[38, 39, 40] and ride-sourcing platforms [41], [42]. It is important to note that road pricing for ride-sourcing platforms is substantially different from other road pricing schemes as it interferes with the complicated interaction among platform pricing, passenger demand and driver supply, which is a unique feature of the ride-sourcing market.

### 3. Optimal Spatial Pricing: Market Equilibrium Model

This section formulates a mathematical model of the optimal spatial pricing problem for a ride-sourcing platform over a transportation network. The model captures the complicated interactions among various endogenous variables, including ride fare, driver payment, passenger and driver distribution, passenger and driver waiting time, vehicle repositioning, traffic congestion, and network flow balance. The details of the model are presented below.

#### 3.1. Problem Setup

Consider a city divided into  $M$  zones. These zones are connected by a road network expressed by a graph  $\mathcal{G}(\mathcal{V}, \mathcal{E})$ , where  $\mathcal{V}$  denotes the set of vertices (or zones) and  $\mathcal{E}$  denotes the set of edges (or roads). We investigate the ride-sourcing market at the zonal granularity, and assign an origin zone  $i \in \mathcal{V}$  and a destination zone  $j \in \mathcal{V}$  to each ride-sourcing trip. Each trip is randomly initiated by a passenger who requests a pickup from zone  $i$  through the user app. Upon receiving the request, the platform matches the passenger to the closest idle vehicle in the same zone<sup>2</sup>, if available. After an idle driver is matched to the passenger, he/she travels to the passenger’s location, picks up the passenger, and then chooses the shortest path from  $i$  to  $j$  to deliver the passenger to the destination. When a trip is completed, the driver can choose either to remain in the same zone or to cruise to a different zone to look for the next passenger. The idle driver remains cruising until he is matched to the next passenger.

#### 3.2. Passenger Model

Passengers make mode choices by comparing the costs of different commute options, such as ride-sourcing, public transit, taxi, and walking. For a passenger traveling from zone  $i$  to zone  $j$ , the generalized cost of the ride-sourcing trip is defined as the weighted sum of the waiting time, the in-vehicle travel time, and the trip fare:

$$c_{ij} = \alpha w_i^p + \beta t_{ij} + r_i t_{ij}, \quad (1)$$

where  $w_i^p$  is the average passenger waiting time in zone  $i$ ,  $r_i$  is the per-time ride fare for trips starting from zone  $i$ ,  $t_{ij}$  is the average trip time from zone  $i$  to zone  $j$ ,  $\alpha$  represents the passenger value-of-time when waiting for the ride, and  $\beta$  represents the passenger’s value of time when traveling on the road. Since travelers typically place a higher value on waiting time [43], we have  $\alpha > \beta$ <sup>3</sup>. It is worth emphasizing that  $t_{ij}$  is an endogenous variable that depends on the traffic flow of the ride-sourcing market (we will delineate this relation in Section 3.4). It is also important to note that  $c_{ij}$  represents the *average* value of the generalized cost, while the travel cost for different passengers can be different due to user heterogeneity and randomness.

---

<sup>2</sup>We assume each passenger is matched to the closest idle vehicle. When vehicles are densely distributed and the zones are reasonably large, there is a high probability that passengers are picked up by idle vehicles in the same zone. This paper exclusively considers this case for simplicity.

<sup>3</sup>The value of passenger waiting time for ridesourcing services may be smaller than that of buses or subway. However, we emphasize that the proposed formulation and solution methodology do not rely on the assumption that  $\alpha > \beta$ .

The passenger waiting time  $w_i^p$  is an endogenous variable that depends on the supply and demand of the ride-sourcing market. Since we have assumed that passengers from zone  $i$  are matched to drivers in the same zone, the passenger waiting time  $w_i^p$  is a monotone function of the average number of idle vehicles (or equivalently, idle vehicle hours  $N_i^I$ ) in zone  $i$ .<sup>4</sup> With slight abuse of notation, we use  $w_i^p(N_i^I)$  to denote this relation. The following assumption is imposed:

**Assumption 1.**  $w_i^p(N_i^I)$  is positive, strictly decreasing with respect to  $N_i^I$ , and  $\lim_{N_i^I \rightarrow 0} w_i^p(N_i^I) = \infty$ .

**Remark 1.** *The structure of the trip fare  $r_i t_{ij}$  closely approximates the industry practice. For instance, both Uber and Lyft have a fixed per-time fare and per-distance fare. They first calculate the total trip fare as the sum of a base fare, a time-based charge, and a distance-based charge, then this total trip fare is multiplied by a surge multiplier that reflects the real-time imbalance between supply and demand in each zone  $i$ . The third term  $r_i t_{ij}$  in (1) can be viewed as an approximation of the total trip fare multiplied by the surge multiplier. This approximation introduces error when the traffic speed is not uniform. However, we believe this is a reasonable simplification. Although adding an extra decision variable to represent the distance-based charge can be addressed by the proposed solution methodology, it would complicate the notation without providing extra insights.*

We assume that passengers choose their transport mode based on the average travel cost of the ride-sourcing trip. The arrival rate of ride-sourcing passengers from zone  $i$  to zone  $j$  is determined by

$$\lambda_{ij} = \lambda_{ij}^0 F_p(c_{ij}), \quad (2)$$

where  $\lambda_{ij}^0$  is the arrival rate of potential passengers from zone  $i$  to zone  $j$  (total travel demand for all transport modes), and  $F_p(\cdot)$  is the proportion of potential passengers who choose to take ride-sourcing. We assume that  $F_p(\cdot)$  is strictly decreasing with respect to the travel cost  $c_{ij}$ . Note that (2) includes the logit model as a special case.

**Remark 2.** *We acknowledge that our model only produces long-term average outcomes for the ride-sourcing market. It does not capture the temporal dynamics (i.e., departure time, arrival time, etc). To address this concern, we can either incorporate the temporal aspect by considering a quasi-static model for each hour, or formulating a fully dynamic model with fine temporal granularity [44]. However, when combined with the ride-sourcing network, both methods may render a much more complex temporal-spatial problem that is difficult to address. For this reason, we leave this as future work.*

### 3.3. Driver Model

In the long-run, drivers are sensitive to earnings and respond to the platform wage by subscribing to or unsubscribing from the platform. In the short-run drivers decide whether to remain in the current zone or cruise to a different zone to look for the next passenger.

The long-term driver decisions determine the total driver or vehicle hours in the overall ride-sourcing network as an increasing function of the average wage offered by the platform. The ride-sourcing vehicle hour is given by

$$N = N_0 F_d(q), \quad (3)$$

where  $N$  is the total vehicle hour,  $q$  is the driver's average hourly wage,  $N_0$  is the supply of potential driver or vehicle hours, and  $F_d(q)$  is a strictly increasing function representing the proportion of drivers willing to subscribe to the ride-sourcing platform at wage  $q$ . Note that (3) includes the logit model as a special case.

---

<sup>4</sup>In this paper, we regard idle vehicle hours as equivalent to the number of idle drivers. It depends on both supply and demand: it increases with respect to driver supply and decreases with respect to passenger demand.

To model short-term driver repositioning decisions, we define  $w_i^d$  as the average driver waiting time in zone  $i$ . By Little's Law, the vehicle idle hour  $N_i^I$  relates to the driver waiting time  $w_i^d$  as

$$N_i^I = w_i^d \sum_{j=1}^N \lambda_{ij}. \quad (4)$$

Drivers make repositioning decisions by comparing his expected earning (per unit time) in each zone. For each trip that originates from zone  $i$ , the average total trip fare depends on the average trip time and the per-time trip fare:

$$\bar{e}_i = r_i \bar{t}_i = r_i \frac{\sum_{j=1}^N \lambda_{ij} t_{ij}}{\sum_{j=1}^N \lambda_{ij}} \quad (5)$$

where  $\bar{e}_i$  is the average trip fare for passengers from zone  $i$ , and  $\bar{t}_i$  is the average trip-time for trips starting from zone  $i$ . Each idle driver can either remain in zone  $i$  or cruise to zone  $j$  to search for the next passenger. If he remains in zone  $i$ , by the end of his next trip, he will experience an average waiting time of  $w_i^d$ , an average trip time of  $\bar{t}_i$ , and earns a proportion<sup>5</sup> of the average total trip fare  $\bar{e}_i$ . In this case, his expected earning (per-unit time) is proportional to  $\frac{\bar{e}_i}{w_i^d + \bar{t}_i}$ . On the other hand, if he cruises to zone  $j$ , by the end of his next trip, he will experience an average waiting time of  $t_{ij} + w_j^d$ , take an average trip time of  $\bar{t}_j$ , and earns a proportion of  $\bar{e}_j$ , which leads to a per-unit time earning that is proportional to  $\frac{\bar{e}_j}{t_{ij} + w_j^d + \bar{t}_j}$ .

Under a logit model, the probability of repositioning from zone  $i$  to zone  $j$  is<sup>6</sup>

$$\left\{ \begin{array}{l} \mathbb{P}_{ij} = \frac{e^{\eta \bar{e}_j / (t_{ij} + w_j^d + \bar{t}_j)}}{\sum_{k \neq i} e^{\eta \bar{e}_k / (t_{ik} + w_k^d + \bar{t}_k)} + e^{\eta \bar{e}_i / (w_i^d + \bar{t}_i)}}, \quad j \neq i, \\ \mathbb{P}_{ii} = \frac{e^{\eta \bar{e}_i / (w_i^d + \bar{t}_i)}}{\sum_{k \neq i} e^{\eta \bar{e}_k / (t_{ik} + w_k^d + \bar{t}_k)} + e^{\eta \bar{e}_i / (w_i^d + \bar{t}_i)}}. \end{array} \right. \quad (6)$$

For each zone  $i$ , the arrival rates of drivers ending their trip is  $\sum_{k=1}^M \lambda_{ki}$ . Since all incoming drivers need to make repositioning decisions, the *intended* vehicle rebalance flow from zone  $i$  to zone  $j$  (or itself) is determined by<sup>7</sup>

$$f_{ij} = \mathbb{P}_{ij} \sum_{k=1}^M \lambda_{ki}. \quad (7)$$

It is important to note that  $f_{ij}$  is only the rebalance flow intended by the driver before he/she actually starts repositioning. During repositioning each vehicle is still available to match a nearby passenger. Therefore, the vehicle can be intercepted by other zones during the transitional period before it reaches the repositioning destination. To capture this, we denote  $\mathcal{P}_{ij} \subset \mathcal{V}$  as the set of zones traversed by the shortest path between zone  $i$  and zone  $j$  (note that  $i, j \in \mathcal{P}_{ij}$ ), and define  $\Pi(k|i \rightarrow j)$  as the probability that a driver is intercepted by zone  $k$  when he is on his way to reposition from zone  $i$  to zone  $j$ . In this case, the resulting rebalancing flow,  $\tilde{f}_{ik}$ , can be derived as

$$\tilde{f}_{ik} = \sum_{j: k \in \mathcal{P}_{ij}} \Pi(k|i \rightarrow j) f_{ij}, \quad (8)$$

<sup>5</sup>The proportion is determined by the commission rate of the platform, which is a uniform number that does not depend on the origin or destination of the trip.

<sup>6</sup>Note that  $\mathbb{P}_{ii}$  differs from  $\mathbb{P}_{ij}$  in that it does not include  $t_{ii}$ . This is because after dropping off the passenger, if the idle driver decides to stay in the same zone, she/he can directly start cruising for the next passenger, thus  $t_{ii}$  should be excluded from his/her cost.

<sup>7</sup>Based on (6), when  $t_{ij}$  is large,  $\mathbb{P}_{ii}$  can be significantly greater than  $\mathbb{P}_{ij}$ . In this case, the majority of the drivers will stay in the same zone to seek the next passenger.

The intercepting probability  $\Pi(k|i \rightarrow j)$  depends on the demand and supply in each zone along the shortest path  $\mathcal{P}_{ij}$ , the sequence of traversing these zones, and the duration that a traversing vehicle stays in these zones. To model this intercepting probability, let us first consider a single zone  $i$  and denote  $d_i$  as the average time spent to traverse zone  $i$ . In this case, an idle driver that traverses zone  $i$  stays in zone  $i$  for an average duration of  $d_i$ . During this period, there is a probability  $\sigma_i$  that the idle vehicle is matched to a passenger before it exits zone  $i$ . To model  $\sigma_i$ , we propose an M/M/1 queue that captures the stochasticity of passengers and drivers in zone  $i$ , where passengers are modeled as servers, and drivers are viewed as jobs. This queuing model has been used in other works modeling the ride-sourcing platforms [45]. Based on the M/M/1 queue, we derive that the waiting time  $\tau$  of the drivers in zone  $i$  is subject to an exponential distribution [46], therefore we have

$$\mathbb{P}(\tau \leq T) = 1 - e^{-T/w_i^d}. \quad (9)$$

Based on (9), if an idle driver stays for a duration of  $d_i$  in zone  $i$ , then the probability that it is matched to a passenger before it exits zone  $i$  is

$$\sigma_i = \mathbb{P}(\tau \leq d_i) = 1 - e^{-d_i/w_i^d} \quad (10)$$

The intercepting probability  $\Pi(k|i \rightarrow j)$  can be derived based on  $\sigma_i$ . In particular, if a repositioning vehicle from zone  $i$  to zone  $j$  is intercepted by zone  $k$ , it indicates that this vehicle is not intercepted by any zones on the shortest path  $\mathcal{P}_{ij}$  prior to zone  $k$ . To make this precise, we order the elements of  $\mathcal{P}_{ij}$  based on the distance to zone  $i$  in an increasing sequence, i.e., the first element  $I_1 \in \mathcal{P}_{ij}$  is zone  $i$  itself, the second element  $I_2 \in \mathcal{P}_{ij}$  is the closest zone to  $i$  on the shortest path  $\mathcal{P}_{ij}$ , the third element  $I_3 \in \mathcal{P}_{ij}$  is the second closest zone to  $i$ , etc. Let  $k$  be the  $s$ th element, which satisfies  $I_s = k$ , then for  $k \neq j$ , the intercepting probability can be derived as:

$$\Pi(k|i \rightarrow j) = (1 - \sigma_{I_1}) \cdot (1 - \sigma_{I_2}) \cdots (1 - \sigma_{I_{s-1}}) \sigma_{I_s}. \quad (11)$$

Equation (11) indicates that if a repositioning vehicle is intercepted by zone  $I_s = k$ , then it must have passed all the zone  $I_1, I_2, \dots, I_{s-1}$  before it enters  $k$ .

**Remark 3.** *The above discussion is based on two underlying assumptions. First, we have assumed that the calculation of  $\sigma_i$  and  $\sigma_j$  are independent. This is a reasonable assumption if we only consider inter-zone matching: the matching radius is smaller than the diameter of each zone, and that each passenger is only matched to a vehicle within the same zone. The case of intra-zone matching [15] is outside the scope of this paper. Second, we assume that when drivers make repositioning decisions based on the logit model (6), they do not anticipate the possibility of being intercepted by other zones. We believe that this is a realistic assumption since the repositioning of human drivers is often guided by intuition instead of computer algorithms. While they can decide the repositioning strategies based on a rough estimate of prospective earnings, they lack the computational resources and the real-time information to carry out more delicate calculations.*

Finally, since each vehicle has three operating modes: (a) carrying a passenger, (b) on the way to pick up the passenger, (c) cruising with empty seats to look for the next passenger, the total number of vehicle hours should be partitioned as

$$N = \sum_{i=1}^M \sum_{j=1}^M \lambda_{ij} t_{ij} + \sum_{i=1}^M \sum_{j=1}^M w_i^p \lambda_{ij} + \sum_{i=1}^M \sum_{j=1}^M w_i^d \lambda_{ij}, \quad (12)$$

where the first term accounts for the operating hours of vehicles with passengers, the second term accounts for the operating hours of vehicles that are on their way to pick up passengers, and the third term accounts for the operating hours of idle vehicles.<sup>8</sup>

---

<sup>8</sup>Note that the vehicle hours associated with the repositioning vehicles are incorporated in the third term of (12) because all repositioning vehicles are available for matching during the repositioning process.

### 3.4. Traffic Congestion

The ride-sourcing vehicles contribute to the traffic congestion of the city. This affects the traffic speed, which further affects the time it takes to travel from zone  $i$  to zone  $j$ . For this reason, the travel time  $t_{ij}$  is an endogenous variable that depends on the spatial distribution of ride-sourcing vehicles. Here we present a traffic congestion model to capture this dependence.

First, we note that the congestion externality of ride-sourcing vehicles is spatially asymmetric: in the core area of the city where streets are already heavily congested, introducing more ride-sourcing vehicles will significantly affect the traffic speed, whereas in remote areas where congestion rarely occurs, ride-sourcing vehicles only have a negligible impact on traffic speed. To model this, we consider a ‘‘congestion area’’  $\mathcal{C} \subset \mathcal{V}$  that consists of all the congested zones in the urban core, and a ‘‘remote area’’ ( $\mathcal{R} = \mathcal{V} \setminus \mathcal{C}$ ) that consists of all other zones in the suburb. Let  $v_c$  and  $v_r$  be the average traffic speed within the congestion area and remote area, respectively. Denote  $d_{ij}$  as the average shortest-path travel distance from zone  $i$  to zone  $j$ . Since a trip from zone  $i$  to zone  $j$  may traverse both  $\mathcal{C}$  and  $\mathcal{R}$ , we denote  $d_{ij}^{\mathcal{C}}$  and  $d_{ij}^{\mathcal{R}}$  as the overlap of  $d_{ij}$  with respect to  $\mathcal{C}$  and  $\mathcal{R}$ , respectively.<sup>9</sup> The travel time  $t_{ij}$  can be then derived as<sup>10</sup>

$$t_{ij} = d_{ij}^{\mathcal{C}} \frac{1}{v_c} + d_{ij}^{\mathcal{R}} \frac{1}{v_r}, \quad (13)$$

where the first term represents the travel time within the congestion area  $\mathcal{C}$  and the second term denotes the travel time within the remote area  $\mathcal{R}$ . We assume that the average travel speed in the remote area does not depend on the ride-sourcing traffic. Therefore, in equation (13),  $d_{ij}^{\mathcal{C}}$ ,  $d_{ij}^{\mathcal{R}}$  and  $v_r$  are all exogenous variables. On the other hand, the traffic speed in the congestion area should depend on the number of ride-sourcing vehicles. Let  $N_{\mathcal{C}}$  denote the total number of ride-sourcing vehicles in the congestion area  $\mathcal{C}$ . With slight abuse of notation, the traffic speed in  $N_{\mathcal{C}}$  can be then denoted as  $v_c(\cdot)$ : a decreasing function of  $N_{\mathcal{C}}$ . Based on equation (13),  $t_{ij}$  is also a function of  $N_{\mathcal{C}}$ .

Finally, the number of ride-sourcing vehicles in  $\mathcal{C}$  should consist of all vehicles traveling in the congestion area, including occupied vehicles that spend a proportion of trip time in  $\mathcal{C}$ , idle vehicles cruising in  $\mathcal{C}$ , and empty vehicles on the way to pick up passengers in  $\mathcal{C}$ . Similar to (12), we have that:

$$N_{\mathcal{C}} = \sum_{i=1}^M \sum_{j=1}^M \lambda_{ij} d_{ij}^{\mathcal{C}} \frac{1}{v_c} + \sum_{i \in \mathcal{C}} \sum_{j=1}^M w_i^p \lambda_{ij} + \sum_{i \in \mathcal{C}} \sum_{j=1}^M w_i^d \lambda_{ij}, \quad (14)$$

where the first term represents all trip times associated with the congestion area,<sup>11</sup> the second term represents all vehicles on the way to pick up the passenger in  $\mathcal{C}$ , and the third term represents all idle cruising vehicles in  $\mathcal{C}$ . Each term in (14) reflects a proportion of the corresponding terms in (12), which is only associated with the congestion area.

**Remark 4.** *Ideally, traffic congestion can be modeled at the zonal level: each zone in the city has its own traffic speed, which depends on the total number of ride-sourcing vehicles in this zone. Our model does not capture congestion at this level of granularity because we primarily focus on congestion charges that differentiate the urban core and the suburb. Therefore, a congestion model at the urban/suburb level already suffices for our purpose. Furthermore, a zonal-level congestion model requires significantly more data (background traffic, road capacity, etc), which is unavailable to us. Therefore, we leave this more detailed congestion model as future work.*

<sup>9</sup>If the trip from  $i$  to  $j$  does not traverse any zone in the congestion area (or remote area), then  $d_{ij}^{\mathcal{C}} = 0$  (or  $d_{ij}^{\mathcal{R}} = 0$ ). In addition, we clearly have  $d_{ij} = d_{ij}^{\mathcal{C}} + d_{ij}^{\mathcal{R}}$ .

<sup>10</sup>We assume that each side of the equation is properly scaled to have the same unit, wherever necessary.

<sup>11</sup>We remind that  $d_{ij}^{\mathcal{C}}/v_c$  is the time spent in the congestion area for a trip from zone  $i$  to zone  $j$ . If a trip does not pass through the congestion area, then we have  $d_{ij}^{\mathcal{C}} = 0$ .

### 3.5. Network Flow Balance

In the long run, the inflow and outflow of vehicles in each zone should be balanced. This leads to the following constraints,

$$\sum_{j=1}^M (\lambda_{ji} + \tilde{f}_{ji}) = \sum_{j=1}^M (\lambda_{ij} + \tilde{f}_{ij}), \quad \forall i \in \mathcal{V}. \quad (15)$$

The left-hand side of (15) denotes the total inflow to zone  $i$  consisting of vehicles with and without passengers, and the right-hand side of (15) denotes the total outflow from zone  $i$  consisting of vehicles with and without passengers. These flows have to be balanced in equilibrium.

### 3.6. Platform Decision Model

Consider a ride-sourcing platform that determines the ride fare  $r_i$  and driver wage  $q$  (or equivalently, a commission rate<sup>12</sup>) to maximize its profit. These decisions are subject to the passenger demand model, driver supply model, driver repositioning model, and the network flow balancing constraints. The optimal spatial pricing problem can be formulated as follows:

$$\max_{\mathbf{r}, q} \sum_{i=1}^M \sum_{j=1}^M r_i t_{ij} \lambda_{ij} - N_0 F_d(q) q \quad (16)$$

$$\left\{ \begin{array}{l} \lambda_{ij} = \lambda_{ij}^0 F_p(\alpha w_i^p(N_i^I) + \beta t_{ij} + r_i t_{ij}) \end{array} \right. \quad (17a)$$

$$w_i^p(N_i^I) \leq w_{max} \quad (17b)$$

$$N_i^I = w_i^d \sum_{j=1}^M \lambda_{ij} \quad (17c)$$

$$N_0 F_d(q) = \sum_{i=1}^M \sum_{j=1}^M \lambda_{ij} t_{ij} + \sum_{i=1}^M \sum_{j=1}^M w_i^p \lambda_{ij} + \sum_{i=1}^M \sum_{j=1}^M w_i^d \lambda_{ij} \quad (17d)$$

$$N_C = \sum_{i=1}^M \sum_{j=1}^M \lambda_{ij} d_{ij}^C \frac{1}{v_c} + \sum_{i \in \mathcal{C}} \sum_{j=1}^M w_i^p \lambda_{ij} + \sum_{i \in \mathcal{C}} \sum_{j=1}^M w_i^d \lambda_{ij} \quad (17e)$$

$$\sum_{j=1}^M (\lambda_{ji} + \tilde{f}_{ji}) = \sum_{j=1}^M (\lambda_{ij} + \tilde{f}_{ij}), \quad i \in \mathcal{V}. \quad (17f)$$

$$\tilde{f}_{ij} = \sum_{k: j \in \mathcal{P}_{ik}} \Pi(j|i \rightarrow k) \mathbb{P}_{ik} \sum_{m=1}^M \lambda_{mi} \quad (17g)$$

where  $\mathbf{r} = (r_1, r_2, \dots, r_M)$ ,  $t_{ij}$  is defined by (13),  $\Pi(j|i \rightarrow k)$  is given by (11), and  $\mathbb{P}_{ik}$  is determined by the logit model (6). The objective function (16) defines the platform profit as the total revenue  $\sum_{i=1}^M \sum_{j=1}^M r_i t_{ij} \lambda_{ij}$  minus the total driver payment  $Nq = N_0 F_d(q)q$ . Constraints (17a)-(17c) specify the passenger demand. Constraint (17b) requires the waiting time in each zone to be smaller than an upper bound.<sup>13</sup> Constraint (17d) combines the driver supply model (3) and the vehicle hour conservation constraint (12). Constraint (17g) is obtained by plugging (7) into (8). The optimal spatial pricing problem

<sup>12</sup>In practice, ride-sourcing platforms often determine a commission rate which indirectly leads to a driver wage  $q$ . However, we note that optimizing over  $q$  is equivalent to optimizing over the commission rate as there is a one-to-one mapping between driver wage  $q$  and the commission rate.

<sup>13</sup>In certain zones of the city, passenger demand is very low, and profit-maximizing decision is to offer no service to this zone. We impose an upper bound on the waiting time to avoid trivial solution arising from this scenario.

is a non-convex program. After the platform specifies the per-time rate  $r_i$  and the driver payment  $q$ , the constraint (17) defines  $M$  endogenous variables  $w_i^d, \forall i \in \mathcal{V}$ . We can substitute (17a)-(17c) into (17d) and substitute (17g) into (17f). Since (17f) only has  $M - 1$  independent constraints,<sup>14</sup> overall (17d) and (17f) constitute  $M$  independent constraints. We further note that given the  $M$  endogenous variables  $w_i^d$ ,  $N_C$  can be derived as a function of these variables through constraint (17e). This further determines  $t_{ij}$  as a function of  $w_i^d$ . Therefore, after plugging  $t_{ij}$  into (17d) and (17f), overall, (17d) and (17f) constitute  $M$  independent constraints for  $M$  endogenous variables when  $r_i$  and  $q$  are given.

**Remark 5.** *Constraint (17b) imposes an upper bound on the pickup time in each zone. This requires the platform to recruit enough drivers to maintain its service quality in all zones, which implicitly places a lower bound on the driver wage  $q$ . However, we comment that the imposition of (17b) is to avoid the trivial case where the platform finds it more profitable to offer no service to some low-demand areas. For this reason, the value of  $w_{max}$  is large (e.g., 10 min) relative to the average pickup time of other zones (e.g., 5 min), thus for most zones the upper bound on the pickup time (17b) is inactive. This implies that the imposition of (17b) will not significantly affect the well-posedness of the optimization problem (16).*

## 4. The Solution Algorithm

This section proposes an algorithm to approximately compute the optimal solutions to (16) and to establish an upper bound to evaluate the performance of the proposed algorithm. Both the algorithm and the upper bound are validated through realistic synthetic ride-sourcing data for San Francisco.

### 4.1. Constraint Relaxation and Upper Bound

The primary constraints in (16) are (17d) and (17f). The vehicle hour balancing constraint (17d) directly relates to driver payment, which has a significant impact on the platform profit. On the other hand, the network flow balance constraint (17f) does not directly affect the profit platform, but only indirectly affects spatial prices by dictating network balance. It is important to note that in a ride-sourcing market, a popular origin is typically also a popular destination (see for example, Figure 1 and Figure 2). For this reason, the incoming passenger flow  $\sum_{j=1}^M \lambda_{ji}$  and outgoing passenger flow  $\sum_{j=1}^M \lambda_{ij}$  in each zone  $i$  are naturally close even without vehicle repositioning. Therefore, we anticipate that relaxing (17f) will not significantly affect the platform's optimal profit. The subsequent discussion is built upon this intuition.

By dropping the network flow balance constraint (17f), the optimal spatial pricing problem (16) can be relaxed to:

$$\max_{\mathbf{r}, \mathbf{N}^I, q} \sum_{i=1}^M \sum_{j=1}^M r_i t_{ij} \lambda_{ij} - N_0 F_d(q) q \quad (18)$$

$$\begin{cases} \lambda_{ij} = \lambda_{ij}^0 F_p(\alpha w_i^p(N_i^I) + \beta t_{ij} + r_i t_{ij}) & (19a) \\ w_i^p(N_i^I) \leq w_{max} & (19b) \end{cases}$$

$$\begin{cases} N_0 F_d(q) = \sum_{i=1}^M \sum_{j=1}^M \lambda_{ij} t_{ij} + \sum_{i=1}^M \sum_{j=1}^M w_i^p \lambda_{ij} + \sum_{i=1}^M N_i^I, & (19c) \end{cases}$$

$$\begin{cases} N_C = \sum_{i=1}^M \sum_{j=1}^M \lambda_{ij} d_{ij}^C \frac{1}{v_c} + \sum_{i \in \mathcal{C}} \sum_{j=1}^M w_i^p \lambda_{ij} + \sum_{i \in \mathcal{C}} N_i^I & (19d) \end{cases}$$

<sup>14</sup>If the balancing constraint holds for  $M - 1$  zones, it automatically holds for the other zone. This is in same spirit as the Walras's law [47].

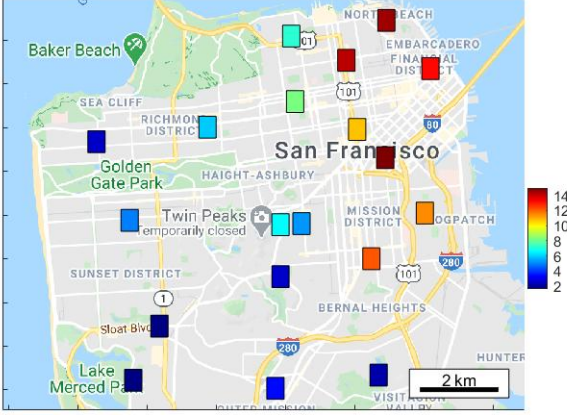


Figure 1: Total inflow per minute to each zip code zone.

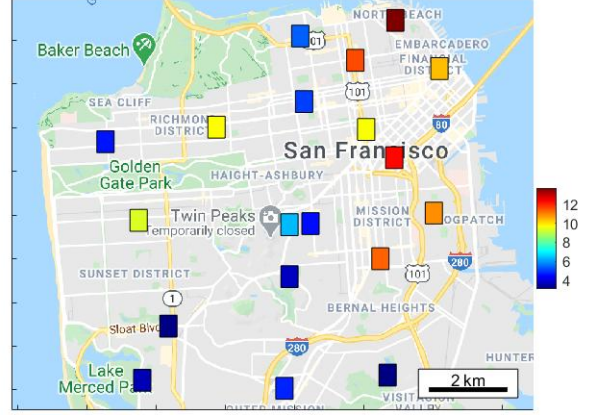


Figure 2: Total outflow per minute from each zip code zone.

where  $\mathbf{N}^I = (N_1^I, N_2^I, \dots, N_M^I)$ , (19c) is derived by substituting (17c) into (17d), and (17g) is removed since  $\tilde{f}_{ij}$  only appears in (17f). In the relaxed problem, since multiple constraints (17f) are removed, it releases more freedom for the platform to make decisions. In this case, the platform has the freedom to place idle vehicles<sup>15</sup> (note that this is not the case for the original problem) and optimize over  $\mathbf{N}^I$ . The optimal value of the relaxed problem (18) provides an upper bound to the optimal spatial pricing problem (16).

#### 4.2. The Solution Algorithm

The relaxed spatial pricing problem (18) has a special structure that is amenable to numerical computation: when  $N_C$  is given, the traffic speed  $v_c$  and the travel times  $t_{ij}$  are uniquely determined. In this case, the decision variables for each zone  $i$ , i.e.,  $r_i$  and  $N_i^I$ , are separable both in the objective function (18) and in the constraints (19c)-(19d). This indicates that the overall problem can be solved by enumerating over  $N_C$  and then performing a dual decomposition under each  $N_C$ . In particular, we first conduct a grid search over the scalar decision variable  $N_C$ . For each  $N_C$ , we dualize (19c) and (19d) to decompose the overall problem into a few optimization problems of much smaller size (e.g., two-dimensional optimization), which can be solved individually and in parallel. In each iteration of the dual-decomposition algorithm, we collect solutions from the decomposed problems to update the dual variable, repeat this calculation until the stopping criterion is satisfied. This entire process is then replicated for a different  $N_C$  until we find the optimal  $N_C$  that leads to the highest platform profit. Since the dual-decomposition step may introduce a non-zero duality gap, the derived solution can be either the exact solution to (18) or an upper bound to (18). In either case, the algorithm provides an upper bound for the original optimal pricing problem (16). Details of the algorithm are summarized in Algorithm 1.

In Algorithm 1, Step 5-Step 9 executes a standard dual-decomposition for the relaxed problem (18). In each iteration, the Lagrangian of (18) is decomposed into decoupled problems (20), (22) and (24), which are small-scale non-convex programs (1D or 2D) that can be efficiently solved to global optimality by brute-force computation. Depending on the duality gap of (18), the termination conditions of the dual-decomposition iteration have two scenarios: (a) there is no duality gap of (18), and the algorithm converges to a solution that satisfies constraints (19c)-(19d); (b) there is a duality gap of (18) and the algorithm terminates to an infeasible point when the algorithm reaches the maximum number of iterations.<sup>16</sup> In either case, the

<sup>15</sup>It is easy to see that optimizing over  $\mathbf{N}^I = (N_1^I, \dots, N_M^I)$  is equivalent to optimizing over  $(w_1^d, \dots, w_M^d)$ .

<sup>16</sup>The platform can terminate the while loop at any time and implement the resulting solution  $\bar{r}$  and  $\bar{q}$ , with  $\bar{R}$  as an upper

---

**Algorithm 1** The solution algorithm for the optimal spatial pricing problem (16)

---

**Initialization:** Initial guess of primal variables  $\bar{\mathbf{r}}, \bar{\mathbf{N}}^{\mathbf{I}}, \bar{q}$ , and dual variables  $\delta, \kappa$ .

- 1: Setup stopping criterion: constraints (19c)-(19d) satisfied or maximum iteration reached.
- 2: **for** each iteration **do**
- 3:   Choose a candidate  $N_{\mathcal{C}}$ ,
- 4:   Calculate  $v_c$  and  $t_{ij}$  based on  $N_{\mathcal{C}}$ ,
- 5:   **while** stopping criterion not satisfied **do**
- 6:     If  $i \in \mathcal{C}$ , solve the decomposed Lagrangian for zone  $i$ :

$$(r_i, N_i^I) = \arg \max_{r_i, N_i^I} \sum_{j=1}^M r_i t_{ij} \lambda_{ij} - \delta \left( \sum_{j=1}^M \lambda_{ij} t_{ij} + \sum_{j=1}^M w_i^p \lambda_{ij} + N_i^I \right) - \kappa \left( \sum_{j=1}^M \lambda_{ij} d_{ij}^{\mathcal{C}} \frac{1}{v_c} + \sum_{j=1}^M w_i^p \lambda_{ij} + N_i^I \right) \quad (20)$$

$$\begin{cases} \lambda_{ij} = \lambda_{ij}^0 F_p(\alpha w_i^p(N_i^I) + \beta t_{ij} + r_i t_{ij}) \end{cases} \quad (21a)$$

$$\begin{cases} w_i^p(N_i^I) \leq w_{max} \end{cases} \quad (21b)$$

If  $i \in \mathcal{R}$ , solve the decomposed Lagrangian for zone  $i$ :

$$(r_i, N_i^I) = \arg \max_{r_i, N_i^I} \sum_{j=1}^M r_i t_{ij} \lambda_{ij} - \delta \left( \sum_{j=1}^M \lambda_{ij} t_{ij} + \sum_{j=1}^M w_i^p \lambda_{ij} + N_i^I \right) - \kappa \sum_{j=1}^M \lambda_{ij} d_{ij}^{\mathcal{C}} \frac{1}{v_c} \quad (22)$$

$$\begin{cases} \lambda_{ij} = \lambda_{ij}^0 F_p(\alpha w_i^p(N_i^I) + \beta t_{ij} + r_i t_{ij}) \end{cases} \quad (23a)$$

$$\begin{cases} w_i^p(N_i^I) \leq w_{max} \end{cases} \quad (23b)$$

- 7:   Solve the decomposed Lagrangian over driver supply,

$$\bar{q} = \arg \max_{q>0} \delta N_0 F_d(q) - N_0 F_d(q) q, \quad (24)$$

- 8:   Update the dual variable

$$\begin{cases} \delta = \delta - \gamma_1 \left( N_0 F_d(q) - \sum_{i=1}^M \sum_{j=1}^M \lambda_{ij} t_{ij} - \sum_{i=1}^M \sum_{j=1}^M w_i^p \lambda_{ij} - \sum_{i=1}^M N_i^I \right) \\ \kappa = \kappa - \gamma_2 \left( N_{\mathcal{C}} - \sum_{i=1}^M \sum_{j=1}^M \lambda_{ij} d_{ij}^{\mathcal{C}} \frac{1}{v_c} - \sum_{i \in \mathcal{C}} \sum_{j=1}^M w_i^p \lambda_{ij} - \sum_{i \in \mathcal{C}} N_i^I \right) \end{cases} \quad (25)$$

- 9:   **end while**

10: **end for**

11: Obtain the solutions  $(\bar{\mathbf{r}}, \bar{\mathbf{N}}^{\mathbf{I}}, \bar{q})$  and the corresponding platform profit  $\bar{R}$ .

12: Use  $(\bar{\mathbf{r}}, \bar{\mathbf{N}}^{\mathbf{I}}, \bar{q})$  as the initial guess to solve (16) using interior-point algorithm, and obtain the solutions  $(\mathbf{r}, \mathbf{N}^{\mathbf{I}}, q)$  and the corresponding platform profit  $R$ .

**Output:** the approximate solution  $(\mathbf{r}, \mathbf{N}^{\mathbf{I}}, q)$ , the corresponding platform profit  $R$  and its upper bound  $\bar{R}$ .

---

algorithm output  $\bar{R}$  provides an upper bound on the optimal value of (16).

**Proposition 1.** *After Algorithm 1 terminates, (a) if constraints (19c)-(19d) are satisfied at  $(\bar{\mathbf{r}}, \bar{\mathbf{N}}^{\mathbf{I}}, \bar{q})$ , then  $(\bar{\mathbf{r}}, \bar{\mathbf{N}}^{\mathbf{I}}, \bar{q})$  is the globally optimal solution to (18), and  $\bar{R}$  is an upper bound on the optimal value of (16); (b) if constraints (19c)-(19d) are not satisfied at  $(\bar{\mathbf{r}}, \bar{\mathbf{N}}^{\mathbf{I}}, \bar{q})$ , then  $(\bar{\mathbf{r}}, \bar{\mathbf{N}}^{\mathbf{I}}, \bar{q})$  is not the globally optimal solution to (18), but  $\bar{R}$  is still an upper bound on the optimal value of (16).*

The proof of Proposition 1 can be found in [48, p.385, p.563], and is therefore omitted. We note that in deriving the optimal spatial prices, the role of the relaxed problem (18) is crucial: its optimizer provides a good initial guess for solving the optimal spatial pricing problem (16), while its optimal value provides an upper bound on the optimality loss.

**Remark 6.** *Although the rebalancing constraint (17f) is relaxed when we compute the upper bound, this relaxation is only performed to provide an initial guess and an upper bound. Ultimately, Algorithm 1 provides a final solution that satisfies all constraints in (17), including the rebalancing constraint (17f). We emphasize that although the rebalancing constraint does not significantly affect the optimal value of the spatial pricing problem, it does affect the optimal solution when we consider the impact of a congestion charge: if (17f) is completely ignored in the model, then very different conclusions will be drawn in Section 5.*

### 4.3. Case Studies

To test the proposed algorithm, we conduct a numerical study using realistic synthetic data for San Francisco. The data consists of the origin and destination of each ride-sourcing trip at the zip-code granularity, which is synthesized based on the total pickup and dropoff in each zone [49] combined with a choice model calibrated by survey data. The zip code zones of San Francisco are shown in Figure 3, and the total passenger inflow (e.g.,  $\sum_{j=1}^M \lambda_{ji}$ ) and outflow (e.g.,  $\sum_{j=1}^M \lambda_{ij}$ ) of each zone are shown in Figure 1 and Figure 2, respectively. Based on the data, we remove zip code zones 94127, 94129, 94130 and 94134 from our analysis since they all have negligible trip volumes. We also aggregate zip code zones 94111, 94104 and 94105 into a single zone, and aggregate 94133 and 94108 into a single zone, since each of these individual zones is very small.

Passenger choice among different transport modes is captured by a logit model, described as

$$\lambda_{ij} = \lambda_{ij}^0 \frac{e^{-\epsilon c_{ij}}}{e^{-\epsilon c_{ij}} + e^{-\epsilon c_{ij}^0}}, \quad (26)$$

where  $\epsilon$  and  $c_{ij}^0$  are model parameters. For driver supply, the long-term driver subscription decisions is captured by

$$N = N_0 \frac{e^{\sigma q}}{e^{\sigma q} + e^{\sigma q_0}}, \quad (27)$$

where  $\sigma$  and  $q_0$  are model parameters.

Assume that the passenger waiting time  $w_i^p$  follows the ‘‘square root law’’ established in [50] and [41]:

$$w_i^p(N_i^I) = \frac{L}{\sqrt{N_i^I}}, \quad (28)$$

where the constant  $L$  depends on the size of the zone and demand/supply distribution. The square root law implies that the average passenger waiting time in zone  $i$  is inversely proportional to the square root

---

bound on its profit.

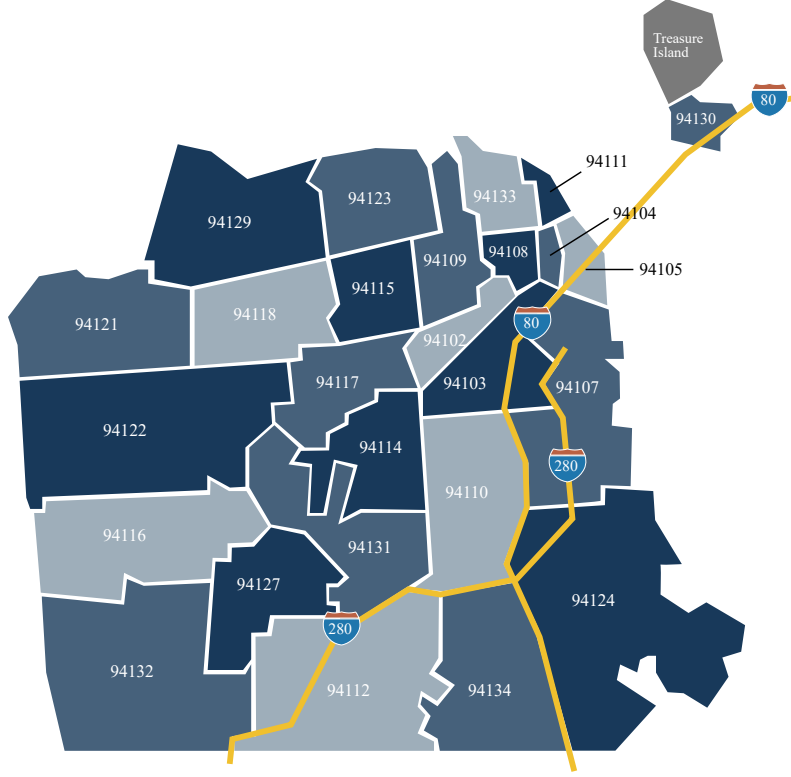


Figure 3: Zip code zones of San Francisco County (figure courtesy: usmapguide.com).

of the number of idle vehicles in zone  $i$ . The intuition behind (28) is that if all idle vehicles are uniformly distributed in zone  $i$ , then the distance between two neighboring idle vehicles is inversely proportional to the square root of the total number of idle vehicles in zone  $i$ . This distance is also proportional to the distance between a passenger and their closest driver, which determines the passenger waiting time.<sup>17</sup> Detailed justification of the square root law can be found in [41].

We further assume that the average value of the inverse of the average traffic speed<sup>18</sup> in the congestion area is a linear function of  $N_C$ , i.e,  $1/v_c = 1/v_c^0 + \rho N_C$ , where  $v_c^0$  and  $\rho$  are model parameters. We emphasize that the choice of this model is only for illustration purpose, which does not affect our methodology or conclusion.

In summary, the model parameters are

$$\Theta = \{\lambda_{ij}^0, N_0, L, \alpha, \beta, \epsilon, \sigma, \eta, c_{ij}^0, q_0, d_{ij}, v_c^0, \rho, v_r\}.$$

The values of these model parameters are set based on data for San Francisco city. In particular,  $\lambda_{ij}^0$  is set to satisfy  $0.15\lambda_{ij}^0 = \lambda_{ij}$  ( $\lambda_{ij}$  is observed from data) so that 15% of the potential passengers take ride-sourcing trips [51]. The travel distance  $d_{ij}$  and traffic speed  $v_r$  are obtained from Google map estimates. The traffic speed model in the congestion area is calibrated so that 1000 ride-sourcing vehicles in the congestion area contributes to 10% reduction of traffic speed (with respect to the traffic speed without ridesourcing vehicles).

<sup>17</sup>The total waiting time for the passenger is the sum of ride confirmation time (from ride request to confirmation) and the pickup time (from ride confirmation to pickup). Typically, the ride confirmation time (e.g., 30 sec) is much shorter than the pickup time (e.g., 5 min) when there is no maximum matching radius and an idle vehicle is always available somewhere. Therefore, in this numerical study we ignore the ride confirmation time and focus on the pickup time.

<sup>18</sup>We choose the inverse of traffic speed (instead of speed) because it is easier to calculate the average trip time  $t_{ij}$  in (13), given that the actual trip time is random across different trips.

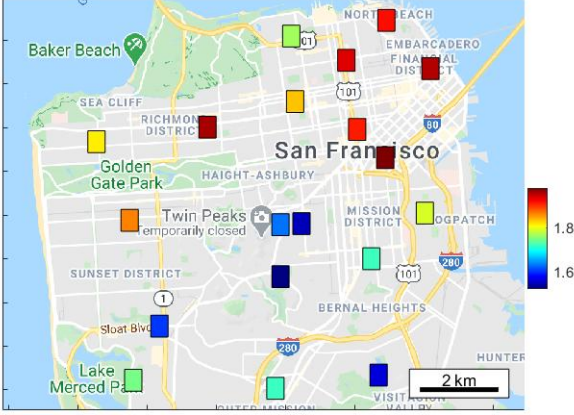


Figure 4: Ride price (\$/min) of ride-sourcing trips.

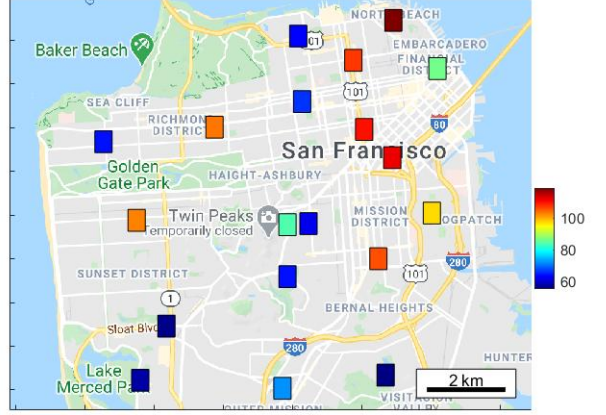


Figure 5: Number of idle vehicles in each zone.

The travel cost of the alternative transport mode  $c_{ij}^0$  (e.g., taxi, buses) is assumed to be proportional to  $d_{ij}$ <sup>19</sup>. To account for unavailability of adequate public transit in remote areas such as zip code zone 94121, 94118, 94125, 94110, 94132, 94112, 94124, we assume that the per-distance cost of alternative transport modes in these areas is 50% higher than in the urban core. The rest of the model parameters are set as

$$N_0 = 10000, L = 43, \alpha = 3, \beta = 1, \epsilon = 0.12, \sigma = 0.17, \eta = 0.1, q_0 = \$29.34/\text{hour},$$

$$w_{max} = 10\text{min}, v_c^0 = 15\text{mph}, \rho = 10\% \frac{1}{v_c^0} \frac{1}{1000}, v_r = 20\text{mph}.$$

These parameter values are adjusted so that the corresponding optimal solution is close to the real-world data of San Francisco (i.e., trip volumes, average trip fare, number of drivers, driver wage, etc). In particular, at the solution to Algorithm 1, passenger arrival rate is 156/min, total number of drivers is 3687, average trip fare is \$17.2/trip, driver wage is \$26.2/hour. The passenger arrival rate and driver supply are consistent with [51] during working hours (e.g., 4PM-5PM) on a typical weekday. The driver wage is close to the estimates<sup>20</sup> (before expense) of [52]. The average trip fare is close to the fare estimates [53] for a 2.6 mile trip [51].

We execute Algorithm 1 using the aforementioned parameter values in Matlab on a Dell desktop machine with 8-core i7-9700 CPU (up to 3.00 GHz), which takes around 196 minutes. At the solution  $(\bar{\mathbf{r}}, \bar{\mathbf{N}}^I, \bar{q})$ , constraints (19c)-(19d) are satisfied. Based on Proposition 1,  $(\bar{\mathbf{r}}, \bar{\mathbf{N}}^I, \bar{q})$  is the globally optimal solution to (18). The optimal value (platform profit) to (18) is \$66,737/hour, while the optimal value of (16), obtained using Algorithm 1, is \$64,749/hour. This indicates that the performance loss of the derived solution is at most 3.1% compared with the globally optimal solution to (16). The ride fare, passenger waiting times, and the distribution of idle ride-sourcing vehicles are shown in Figure 4-Figure 7. The spatial distribution of the ride-sourcing market is unbalanced: the urban core with its high demand zones (zip code zones

<sup>19</sup>By considering  $c_{ij}^0$  as a function of  $d_{ij}$ , it is inherently assumed that alternative transport options are not subject to traffic congestion. This assumption applies to many transport modes, such as buses with dedicated lanes, subway, walking, biking, etc. These modes altogether serve a lion's share of the overall mobility needs. Therefore, it is reasonable to assume that ride-hailing passengers are primarily choosing between TNC and these congestion-independent transport options.

<sup>20</sup>It is estimated that the before expense earning of ride-sourcing drivers in NYC is \$25.76/hour after the minimum wage regulation [51]. The minimum wage in SF is \$0.59 higher than that of NYC, so we estimate that driver wage in SF is 26.35/hour. This is close to the result of our numerical study.

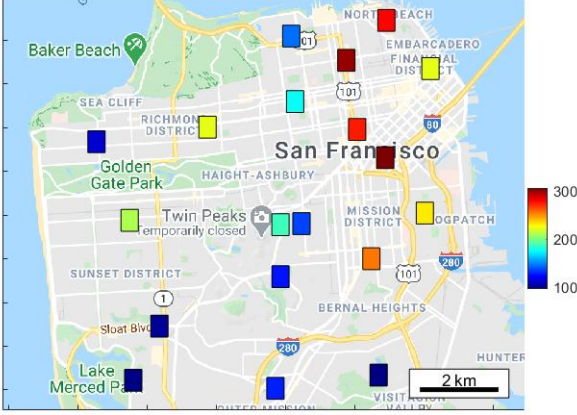


Figure 6: Total number of vehicles in each zone.

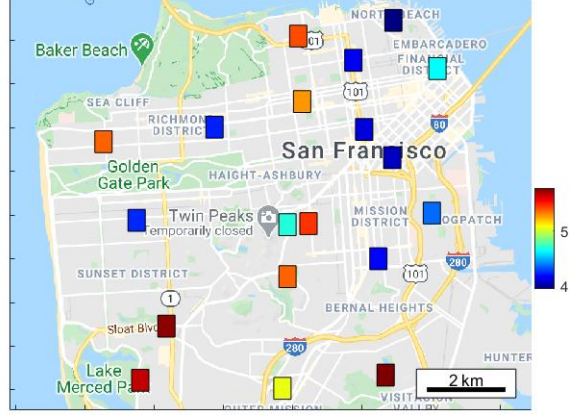


Figure 7: Passenger waiting time (min) in each zone.

94102, 94103, 94104, 94105, 94107, 94108, 94109, 94111, 94133) faces high trip fares (Figure 4) and low waiting times (Figure 7), while suffering greater congestion (13.5mph in  $\mathcal{C}$  v.s. 20mph in  $\mathcal{R}$ ) from attracting idle ride-sourcing vehicles: based on Figure 5, more than 44% of the idle vehicles are concentrated in the northeast corner of the city, which only accounts for 18% of the total area.

To investigate how model parameters affect the performance of Algorithm 1, we conduct a sensitivity analysis by perturbing the parameter values of  $\alpha$ ,  $\epsilon$ ,  $\sigma$ ,  $\eta$ ,  $N_0$  and  $\lambda_0$  in both directions by 30%. Each of the selected parameters is perturbed one by one while other parameters are fixed at their nominal values. Since  $\lambda_0$  is a matrix, we perturb all entries of  $\lambda_0$  proportionately. The upper bound on the performance loss is defined as  $\frac{\bar{R} - R}{\bar{R}}$ , where  $R$  represents the (potentially suboptimal) platform profits of (16) and  $\bar{R}$  represents the platform profits of (18), both evaluated at the solutions to Algorithm 1. The numerical results are shown in Figure 44-Figure 49 (Appendix A). It is clear that the upper bound on the performance loss is consistently small for a large range of model parameters.

## 5. Impacts of Congestion Charges

Our numerical study so far suggests that the spatial distribution of the ride-sourcing vehicles is highly unbalanced. Idle drivers prefer to cruise in the urban core to pick up the next passenger within a shorter time, which leads to the flooding of ride-sourcing vehicles in the urban core and limited availability of ride-sourcing services in remote areas. This section explores regulatory policies that limit congestion in the urban core and benefit travelers in remote areas.

### 5.1. Optimal Pricing under a Congestion Charge

To limit traffic in the congestion area, we consider three forms of congestion charge: (a) a one-directional charge on all vehicles that enter the congestion zone; (b) a bi-directional charge on all vehicles that either enter or exit the congestion zone; (c) a congestion charge on all ride-sourcing trips. The first two congestion charges are cordon-based, which impose a per-crossing fare on all vehicles that cross the cordon regardless of whether there is a passenger on-board. We assume that when an occupied vehicle passes the cordon,

the congestion charge is paid by the passenger,<sup>21</sup> whereas for idle vehicles that pass the cordon, the extra charge is paid by the driver.<sup>22</sup> On the other hand, the third congestion charge is trip-based, which imposes a charge only on passengers and does not penalize idle vehicles. We define  $\bar{p}_{ij}$  as the congestion charge on vehicles that travel from  $i$  to  $j$ , and denote  $\mathbb{1}_{ij}^p$  and  $\mathbb{1}_{ij}^d$  as an indicator function to represent whether the charge is imposed on passengers or drivers, respectively. The optimal spatial pricing problem can be written as

$$\max_{\mathbf{r}, \mathbf{q}} \sum_{i=1}^M \sum_{j=1}^M r_i t_{ij} \lambda_{ij} - N_0 F_d(q) q - \sum_{i=1}^M \sum_{j=1}^M \tilde{f}_{ij} \mathbb{1}_{ij}^d \bar{p}_{ij} \quad (29)$$

$$\left\{ \begin{array}{l} \lambda_{ij} = \lambda_{ij}^0 F_p \left( \alpha w_i^p (N_i^I) + r_i t_{ij} + \beta t_{ij} + \bar{p}_{ij} \mathbb{1}_{ij}^p \right) \end{array} \right. \quad (30a)$$

$$w_i^p (N_i^I) \leq w_{max} \quad (30b)$$

$$N_i^I = w_i^d \sum_{j=1}^M \lambda_{ij} \quad (30c)$$

$$N_0 F_d(q) = \sum_{i=1}^M \sum_{j=1}^M \lambda_{ij} t_{ij} + \sum_{i=1}^M \sum_{j=1}^M w_i^p \lambda_{ij} + \sum_{i=1}^M \sum_{j=1}^M w_i^d \lambda_{ij}, \quad (30d)$$

$$N_c = \sum_{i=1}^M \sum_{j=1}^M \lambda_{ij} d_{ij}^c \frac{1}{v_c} + \sum_{i \in \mathcal{C}} \sum_{j=1}^M w_i^p \lambda_{ij} + \sum_{i \in \mathcal{C}} \sum_{j=1}^M w_i^d \lambda_{ij} \quad (30e)$$

$$\sum_{j=1}^M (\lambda_{ji} + \tilde{f}_{ji}) = \sum_{j=1}^M (\lambda_{ij} + \tilde{f}_{ij}), \quad \forall i \in \mathcal{V}. \quad (30f)$$

$$\tilde{f}_{ij} = \sum_{k: j \in \mathcal{P}_{ik}} \Pi(j|i \rightarrow k) \tilde{\mathbb{P}}_{ik} \sum_{m=1}^M \lambda_{mi} \quad (30g)$$

In (30g), the modified driver repositioning probability  $\tilde{\mathbb{P}}_{ij}$  under congestion charge is defined as

$$\left\{ \begin{array}{l} \tilde{\mathbb{P}}_{ij} = \frac{e^{\eta(\bar{e}_j - \mathbb{1}_{ij}^d \bar{p}_{ij}) / (t_{ij} + w_j^d + \bar{t}_j)}}{\sum_{k \neq i} e^{\eta(\bar{e}_k - \mathbb{1}_{ik}^d \bar{p}_{ik}) / (t_{ik} + w_k^d + \bar{t}_k)} + e^{\eta \bar{e}_i / (w_i^d + \bar{t}_i)}}, \quad j \neq i, \\ \tilde{\mathbb{P}}_{ii} = \frac{e^{\eta \bar{e}_i / (w_i^d + \bar{t}_i)}}{\sum_{k \neq i} e^{\eta(\bar{e}_k - \mathbb{1}_{ik}^d \bar{p}_{ik}) / (t_{ik} + w_k^d + \bar{t}_k)} + e^{\eta \bar{e}_i / (w_i^d + \bar{t}_i)}}. \end{array} \right. \quad (31)$$

Note that when the congestion charge is imposed on passengers, it enters the passenger travel cost and modifies the demand function (30a), whereas when it is imposed on idle vehicles, it enters both driver repositioning model (31) and the driver supply model (30d). However, to simplify the notation, we include the congestion charge (on idle drivers) as the third term of the objective function (29) instead of in (30d). We comment that these two formulations are mathematically equivalent: by a change of variable, we can prove that subtracting a total congestion charge from the platform's objective (29) is equivalent to subtracting a per-driver congestion charge from the driver supply function (30d) [54, Chap. 16].

Let  $\mathbb{1}^p$  and  $\mathbb{1}^d$  denote the matrix form of the indicator functions, where the  $i$ th row and  $j$ th column is  $\mathbb{1}_{ij}^p$  and  $\mathbb{1}_{ij}^d$ , respectively. We have the following three cases:

<sup>21</sup>The platform typically passes the congestion charge to passengers by adding an extra fee on top of the total trip fare. This is consistent with our formulation. We would like to emphasize that in the long term, the platform will need to adjust the ride fare and ultimately the tax burden is shared between the platform and the passengers depending on demand elasticity.

<sup>22</sup>We envision that when a congestion charge is imposed on idle vehicles, the ride-sourcing platform will also pass the extra charge to drivers, just like it did to passengers.

- for one-directional congestion charge,  $\mathbb{1}^p$  and  $\mathbb{1}^d$  are defined as

$$\mathbb{1}_{ij}^p = \mathbb{1}_{ij}^d = \begin{cases} 1, & \text{if } i \in \mathcal{R} \text{ and } j \in \mathcal{C} \\ 0, & \text{Otherwise} \end{cases} \quad (32)$$

- for bi-directional congestion charge,  $\mathbb{1}^p$  and  $\mathbb{1}^d$  are defined as

$$\mathbb{1}_{ij}^p = \mathbb{1}_{ij}^d = \begin{cases} 1, & \text{if } i \in \mathcal{R} \text{ and } j \in \mathcal{C} \\ 1, & \text{if } i \in \mathcal{C} \text{ and } j \in \mathcal{R} \\ 0, & \text{Otherwise} \end{cases} \quad (33)$$

- for trip-based congestion charge,  $\mathbb{1}^p$  and  $\mathbb{1}^d$  are defined as

$$\mathbb{1}_{ij}^p = 1, \quad \mathbb{1}^d = 0. \quad (34)$$

In all cases, the optimal spatial pricing problem under the congestion charge is a non-convex program. The optimal solution to (29) and the upper bound can be obtained by Algorithm 1.

## 5.2. Case Studies

We present a case study for San Francisco to evaluate the impacts of congestion charges on the ride-sourcing market. The northeast corner of San Francisco is the most congested area. Therefore, we define the congestion area  $\mathcal{C}$  as consisting of zip code zones 94111, 94104, 94105, 94133, 94108, 94109, 94102, 94103 and 94107 (see Figure 3). In the case study, we will use the same passenger demand model, driver supply model, and pickup time model as in (26), (27), and (28), respectively. We will also use the same set of model parameters as in Section 4.3 and solve the optimal spatial pricing problem (29) based on Algorithm 1. The algorithm was executed in Matlab on a Dell desktop machine with 8-core i7-9700 CPU (up to 3.00 GHz). A few sets of simulation results will be presented, including (a) the spatial distribution of ride-sourcing vehicles, passenger demand and ride fare before and after a congestion charge of  $\bar{p}_{ij} = \$3$ ; (b) comparison of distinct congestion charge schemes in terms of congestion mitigation, tax revenue, and tax incidence; (c) sensitivity analysis that investigates how model parameters affect the insights and conclusions.

### 5.2.1. Spatial distribution before and after the congestion charge

We first compare the spatial distribution of supply and demand in the ride-sourcing market before and after a congestion charge of  $\bar{p}_{ij} = \$3$ . The comparison is performed for each congestion charge scheme, and the *changes* (in percentage) in vehicle distributions, ride fare, and passenger demand are summarized in Figure 8-22. The numerical values are shown in Table 2-4 in Appendix C.

Figure 8-12 show the impact of the one-directional cordon price. These results provide a few interesting insights, which are listed below:

- It is clear that the one-directional cordon price reduces the number of idle vehicles in the congestion area (see Figure 8) and thus reduces the total ride-sourcing traffic in the urban core (see Figure 9).
- The number of idle vehicles in some of the remote zones increases (Figure 8). This indicates that the waiting time in those areas reduces and the service quality is improved. We point out that this is partially because the one-directional cordon price discourages idle drivers from entering the congestion area and motivates them to serve more passengers in the underserved zones. Furthermore, Figure



Figure 8: % Change in idle driver distribution after the one-directional cordon charge of \$3.

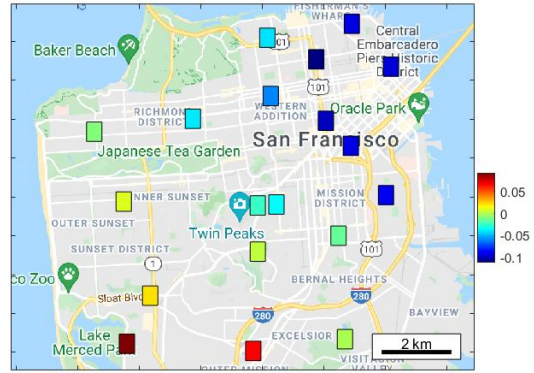


Figure 9: % Change in total number of vehicles after the one-directional cordon charge of \$3.

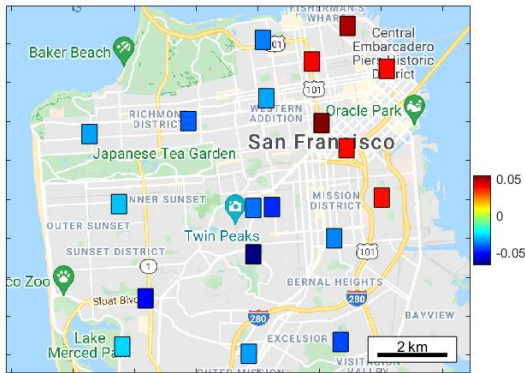


Figure 10: % Change in ride fare after the one-directional cordon charge of \$3.

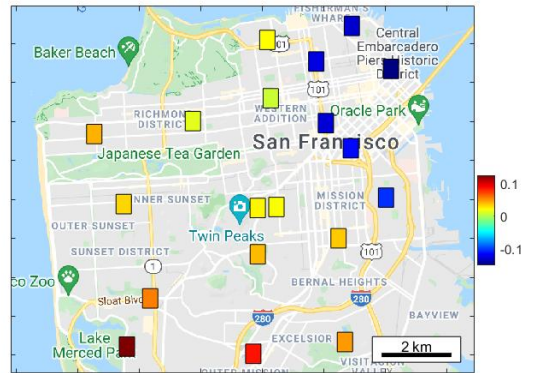


Figure 11: % Change in outflow to uncongested area after the one-directional cordon charge of \$3.

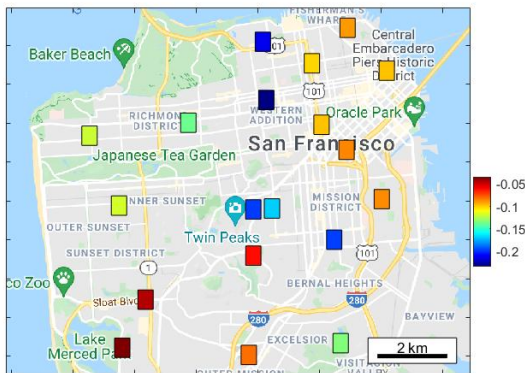


Figure 12: % Change in outflow to congested area after the one-directional cordon charge of \$3.



Figure 13: % Change in idle driver distribution after the bi-directional cordon charge of \$3.

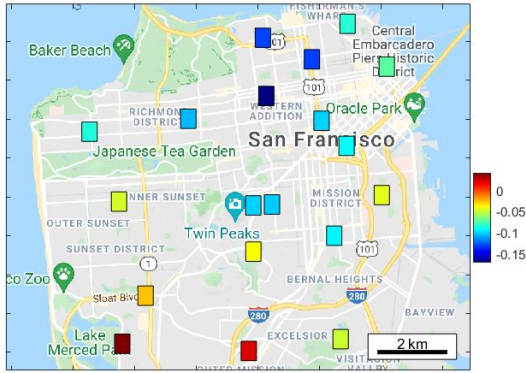


Figure 14: % Change in total number of vehicles after the bi-directional cordon charge of \$3.

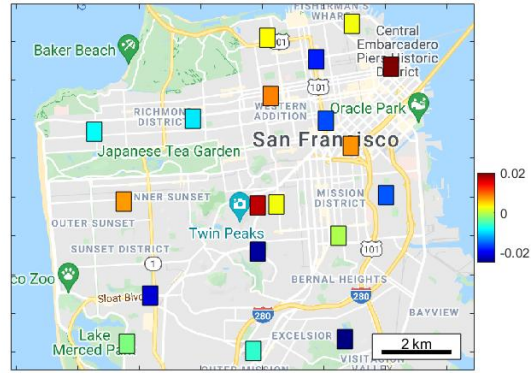


Figure 15: % Change in ride fare after the bi-directional cordon charge of \$3.

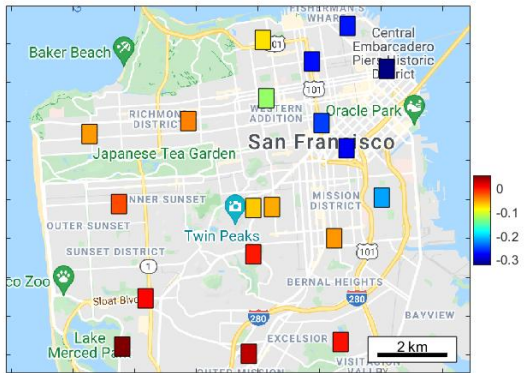


Figure 16: % Change in outflow to uncongested area after the bi-directional cordon charge of \$3.



Figure 17: % Change in outflow to congested area after the bi-directional cordon charge of \$3.



Figure 18: % Change in idle driver distribution after the trip-based charge of \$3.

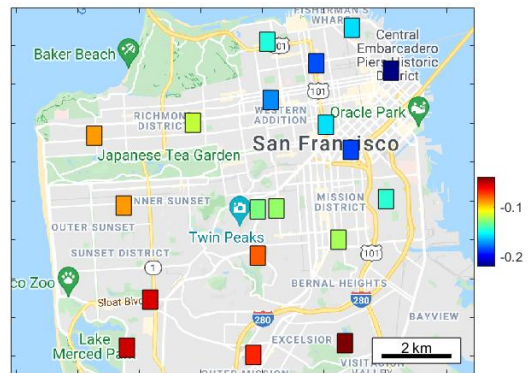


Figure 19: % Change in total number of vehicles after the trip-based charge of \$3.

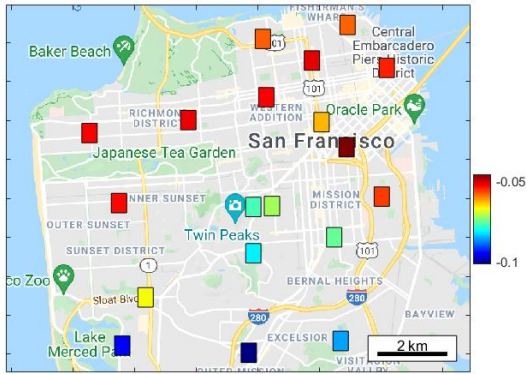


Figure 20: % Change in ride fare after the trip-based charge of \$3.

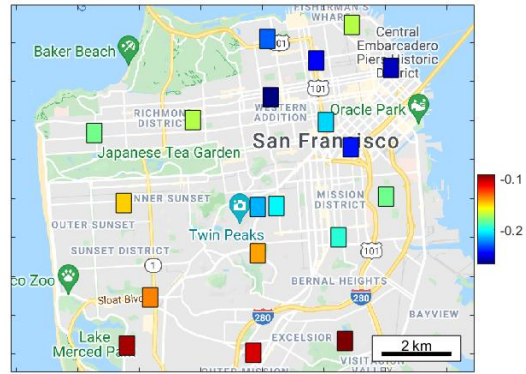


Figure 21: % Change in outflow to uncongested area after the trip-based charge of \$3.

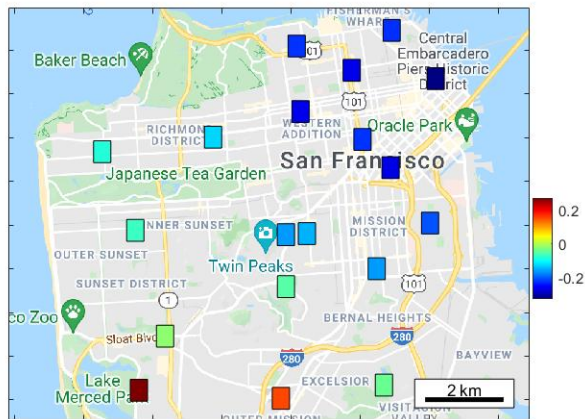


Figure 22: % Change in outflow to congested area after the trip-based charge of \$3.

10 shows that under the one-directional cordon price, the ride fare in the remote area decreases.<sup>23</sup> Together with the increased number of idle vehicles, this indicates that the generalized travel cost for passengers starting from the remote area reduces, leading to higher passenger demand in  $\mathcal{R}$  (see Figure 11).

- In Figure 8 and Figure 11, we observe that zones further from the congestion area benefit more than zones closer to the congestion area. We validate that this is because those zones have fewer trips to the congestion area, so that they are less affected by the cordon charge.
- In Figure 10 and Figure 11, the ride fare in the congestion area increases and the passenger trips from the congestion area to the remote area significantly reduce. This is somewhat surprising because these trips are not directly penalized under the one-directional cordon price. We conjecture that this is because each trip from the congestion area to the remote area would necessitate some rebalancing flow back to the congestion area, which incurs an extra charge for passing the cordon in the future.

Figures 13-17 show the impact of the bi-directional cordon price on the ride-sourcing market. The bi-directional cordon price discourages passengers and vehicles from moving between the congested and uncongested areas. Therefore, cross-cordon trips are severely penalized and the corresponding demand reduces (Figure 16-17). It is interesting to note that the impact of the bi-directional cordon price on each zone depends on how many trips starting from this zone cross the cordon. If the percentage of cross-cordon trips is small, then the congestion charge may have a smaller impact. For instance, we observe that for very remote zones that are far from the cordon, the number of idle vehicles may increase (see Figure 13) and the trip fare may reduce (see Figure 15), which benefits passengers in these zones. It is also interesting to observe that although trips that cross the cordon are penalized and the corresponding demand reduces, trips that do not cross the cordon are not significantly affected, and the corresponding demands for these trips even increases in certain zones (Figure 16-17).

Figures 18-22 show the impact of the trip-based congestion charge on the ride-sourcing market. The trip-based congestion charge penalizes all trips in the city, which curbs the overall ride-sourcing demand and reduces the market size. However, it is interesting to note that since the congestion area has a much larger demand, it assumes a larger tax incidence than other zones in the remote area. For instance, in the congestion area, the number of ride-sourcing vehicles is reduced (Figure 18 and Figure 19), and the passenger demand is curbed (Figure 21 and Figure 22). At the same time, in some zones of the remote area, the number of vehicles increases (Figure 18 and Figure 19), the trip fare reduces (Figure 20), and the trip volume also increases (Figure 22).

### 5.2.2. Comparing distinct schemes of congestion charges

The simulation results in Section 5.2.1 provide a snapshot of the ride-sourcing network at two specific values of  $\bar{p}_{ij}$ . To better compare distinct congestion charge schemes, here we will continuously adjust  $\bar{p}_{ij}$  and calculate the aggregated market outcomes in the congestion area and the remote area for the three congestion charge schemes, respectively.

Figures 23-34 show the simulation results as we vary the congestion charge  $\bar{p}_{ij}$  from \$0/vehicle (or trip) to \$3/vehicle (or trip). For notation convenience, we denote  $\lambda_{11}$  as the total trip flow from  $\mathcal{C}$  to  $\mathcal{C}$ ,  $\lambda_{12}$  as the total trip flow from  $\mathcal{C}$  to  $\mathcal{R}$ ,  $\lambda_{21}$  as the total trip flow from  $\mathcal{R}$  to  $\mathcal{C}$ , and  $\lambda_{22}$  as the total trip flow from  $\mathcal{R}$

<sup>23</sup>Note that the ride fare  $r_i$  shown in Figure 10, Figure 15 and Figure 20 do not include the cordon charge for trips entering the congestion area.

<sup>24</sup>Vehicle occupancy is calculated by dividing the number of occupied vehicles by the total number of vehicles (including all vehicles that are either occupied, idle, or on the way to pick up passengers.)

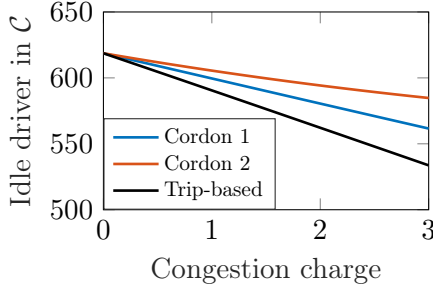


Figure 23: Number of idle drivers in  $\mathcal{C}$  under different surcharge  $\bar{p}_{ij}$ .

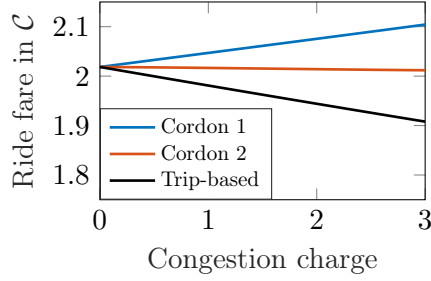


Figure 24: Average ride fare in  $\mathcal{C}$  under different surcharge  $\bar{p}_{ij}$ .

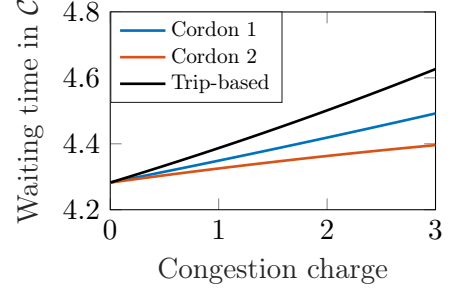


Figure 25: Average passenger waiting time in  $\mathcal{C}$  under different surcharge  $\bar{p}_{ij}$ .

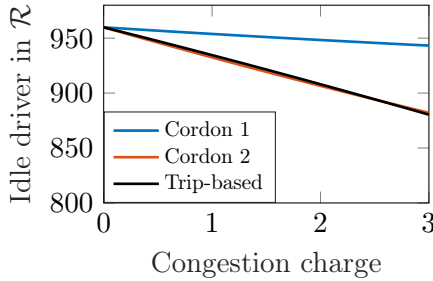


Figure 26: Number of idle drivers in  $\mathcal{R}$  under different surcharge  $\bar{p}_{ij}$ .

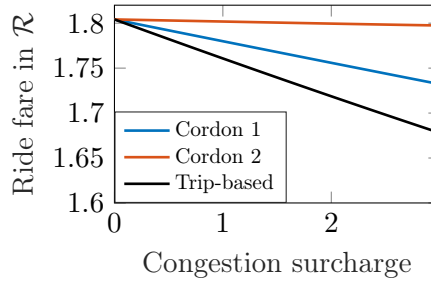


Figure 27: Average ride fare in  $\mathcal{R}$  under different surcharge  $\bar{p}_{ij}$ .

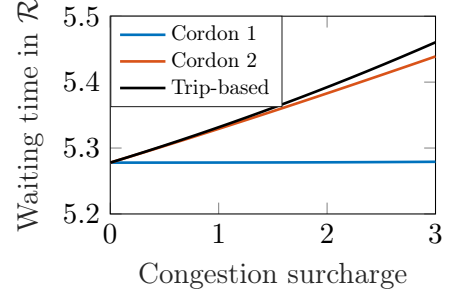


Figure 28: Average passenger waiting time in  $\mathcal{R}$  under different surcharge  $\bar{p}_{ij}$ .

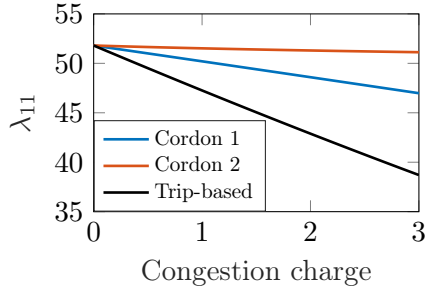


Figure 29: Trips from  $\mathcal{C}$  to  $\mathcal{C}$ ,  $\lambda_{11}$ , under different surcharge  $\bar{p}_{ij}$ .

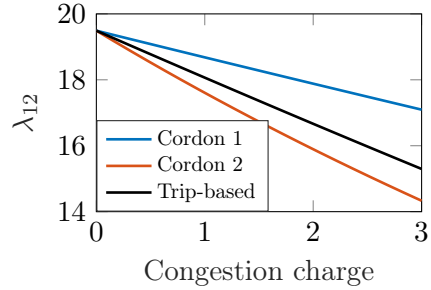


Figure 30: Trips from  $\mathcal{C}$  to  $\mathcal{R}$ ,  $\lambda_{12}$ , under different surcharge  $\bar{p}_{ij}$ .

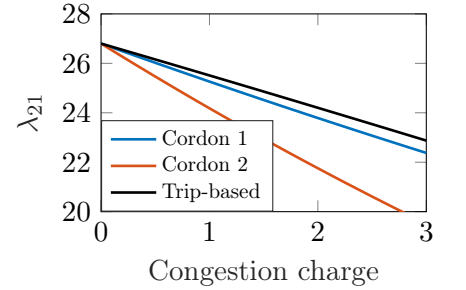


Figure 31: Trips from  $\mathcal{R}$  to  $\mathcal{C}$ ,  $\lambda_{21}$ , under different surcharge  $\bar{p}_{ij}$ .

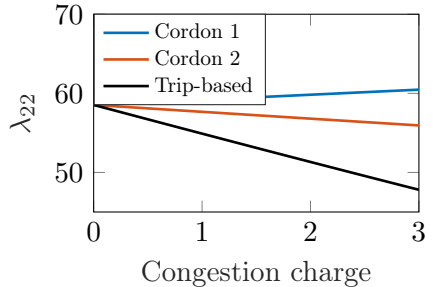


Figure 32: Trips from  $\mathcal{R}$  to  $\mathcal{R}$ ,  $\lambda_{22}$ , under different surcharge  $\bar{p}_{ij}$ .

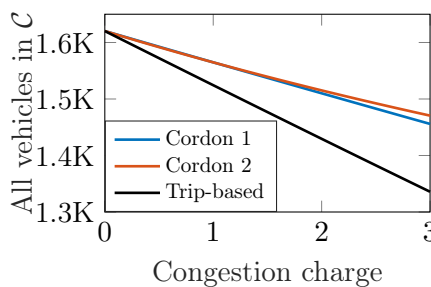


Figure 33: Total number of drivers in  $\mathcal{C}$  under different surcharge  $\bar{p}_{ij}$ .

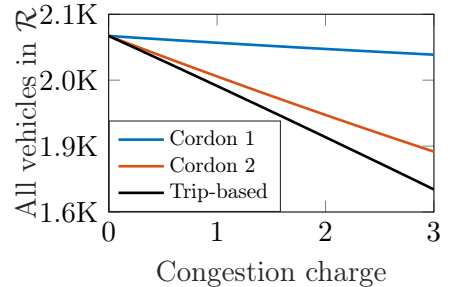


Figure 34: Total number of drivers in  $\mathcal{R}$  under different surcharge  $\bar{p}_{ij}$ .

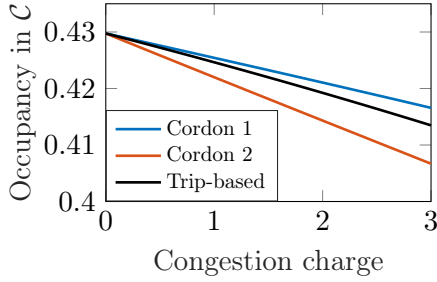


Figure 35: Vehicle occupancy<sup>24</sup> in  $\mathcal{R}$  under different surcharge  $\bar{p}_{ij}$ .

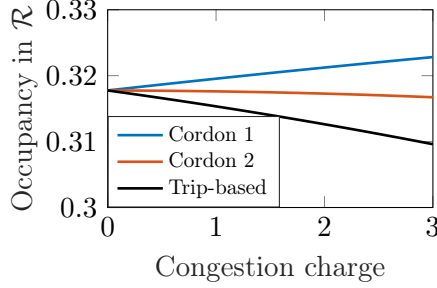


Figure 36: Vehicle occupancy in  $\mathcal{C}$  under different surcharge  $\bar{p}_{ij}$ .

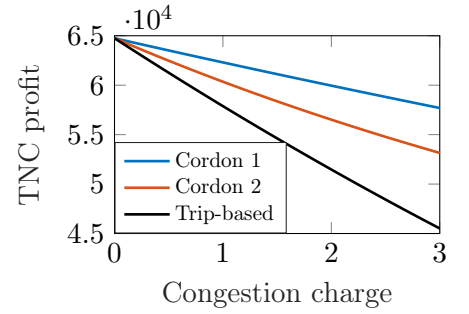


Figure 37: Platform profit per hour under different surcharge  $\bar{p}_{ij}$ .

to  $\mathcal{R}$ . In the figure legend, “Cordon 1” represents the one-directional cordon price, “Cordon 2” represents the bi-directional cordon price, and “Trip-based” represents the trip-based congestion charge. In all cases, the number of idle vehicles and the total number of vehicles (including idle vehicles, occupied vehicles,<sup>25</sup> and vehicles on the way to pick up passengers) in the congestion area is reduced (Figure 23 and Figure 33). Passengers in  $\mathcal{C}$  bear the congestion charge and shift to other transport modes due to the increased overall travel cost associated with ride-sourcing trips (Figure 29 and Figure 30). This further confirms that all forms of congestion charge are effective in reducing the number of ride-sourcing vehicles and alleviating traffic congestion in  $\mathcal{C}$ .

Based on the simulation results, we note that the one-directional cordon price not only limits congestion in the congestion area but also benefits passengers in the remote area. After the one-directional cordon price is imposed, the average ride fare of the remote area reduces<sup>26</sup> (Figure 27), and the average waiting time also decreases (Figure 28).<sup>27</sup> Therefore, the number of trips from the remote area to the remote area increases (Figure 32), and the surplus of passengers in these underserved zones is improved. For this reason, the one-directional cordon price is distinguished from the other congestion charge schemes as it can reduce congestion and promote equity at the same time.

A congestion charge can achieve two objectives: (a) reduce the traffic congestion in the urban core, and (b) raise revenue to subsidize public transit. To evaluate the effectiveness of different congestion charge schemes in achieving these two goals, we conduct the following two sets of experiments:

- First, we measure traffic congestion in the congestion area by the total number of ride-sourcing vehicles within  $\mathcal{C}$ , i.e.,  $N_{\mathcal{C}}$ . To compare the performance of different congestion charges in congestion mitigation, we set a reduction target of  $\Delta N_{\mathcal{C}}$  for  $N_{\mathcal{C}}$ , and compare the passenger surplus, driver surplus and platform profit of these congestion charge schemes when they achieve the same level of traffic reduction  $\Delta N_{\mathcal{C}}$ . Figure 38-40 show the comparison of passenger demand, driver supply, and platform profit, respectively, for different values of  $\Delta N_{\mathcal{C}}$ . It is evident that to achieve the same traffic reduction in  $\mathcal{C}$ , the one-directional cordon price leads to consistently higher passenger surplus, higher driver surplus, and higher platform profit than other congestion charges. We comment that this is because the one-directional cordon price can more precisely target at reducing traffic in the congestion area: (a) compared to the bi-directional cordon price, the one-directional cordon price only

<sup>25</sup>For occupied vehicles traveling from zone  $i$  to zone  $j$ , we evenly distribute the vehicle time to all zones along the shortest path from  $i$  to  $j$ .

<sup>26</sup>Note that the ride fare  $r_i$  shown in Figure 24 and Figure 27 do not include the cordon surcharge for trips entering the congestion area.

<sup>27</sup>Note that in Figure 26, the total number of idle drivers in the remote area decreases. This does not conflict with the reduced average waiting time in Figure 28 because the waiting time in certain zones of the remote area reduces, while the waiting time in other zones increases. Its average value may either increase or decrease, depending on the model parameters.

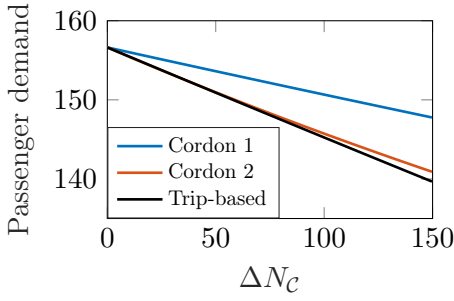


Figure 38: Total trip volumes per minute under different target of traffic reduction in  $\mathcal{C}$ .

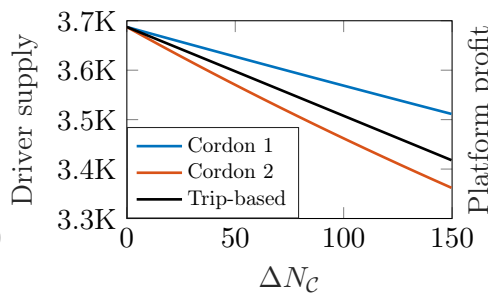


Figure 39: Total number of drivers under different target of traffic reduction in the congestion area  $\mathcal{C}$ .

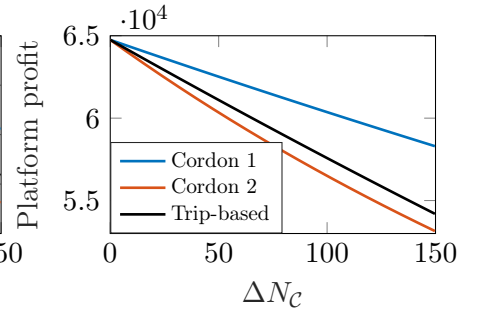


Figure 40: Platform profit per hour under different target of traffic reduction in  $\mathcal{C}$ .

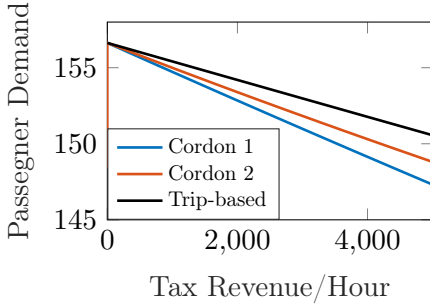


Figure 41: Total trip volumes per minute under different target of tax revenue.

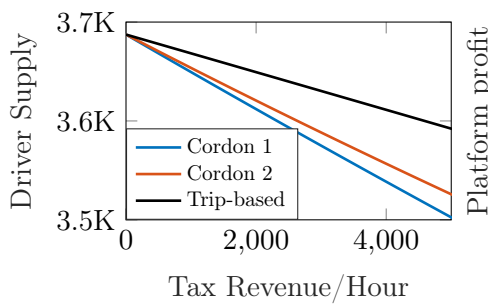


Figure 42: Total number of drivers under different target of tax revenue.

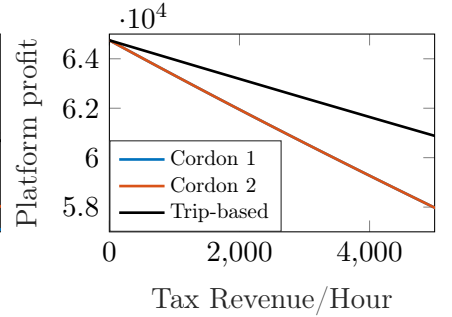


Figure 43: Platform profit per hour under different target of tax revenue.

penalizes vehicle flow that deteriorates the traffic congestion in  $\mathcal{C}$  (i.e., from  $\mathcal{R}$  to  $\mathcal{C}$ ), and does not penalize vehicle flow that mitigates the traffic congestion in  $\mathcal{C}$  (i.e., from  $\mathcal{C}$  to  $\mathcal{R}$ ); (b) compared to the trip-based congestion charge, the one-directional cordon price not only penalizes occupied flows that contribute to the traffic congestion in  $\mathcal{C}$ , but also penalizes idle vehicles that intend to enter the congestion area. For these reasons, the one-directional cordon price can very precisely target at reducing  $N_{\mathcal{C}}$  and achieve the same level of traffic reduction at a smaller cost to passengers, drivers and the platform.

- Second, to compare the performances of distinct congestion charges in revenue-raising, we set a tax revenue target and compare the passenger surplus, driver surplus and platform profit of these congestion charge schemes when they achieve the same tax revenue. Figure 41-43 show the comparison of passenger demand, driver supply, and platform profit, respectively, for different values of the tax target. It is clear that the trip-based congestion charge is most effective in revenue-raising: to achieve the same tax revenue, the trip-based charge leads to higher passenger surplus, higher driver surplus, and higher platform profit than other congestion charges. This is intuitive as the trip-based congestion charge is imposed on the largest number of trips and enjoys the largest base. Therefore, it is more effective in revenue-raising than the other two congestion charge schemes.

To further investigate how the tax burden is distributed among passengers, drivers, and the ride-sourcing platform, we fix the congestion charge level at \$3/trip for all the three schemes, and compute the passenger surplus, driver surplus, platform profit, and tax revenue under the three schemes. The results are summarized in Table 1.<sup>28</sup> Under the same congestion charge level, the trip-based congestion charge has the largest tax revenue and the largest impact on passenger surplus, driver surplus and platform profit. It

<sup>28</sup>The unit of passenger surplus, driver surplus, platform profit and tax revenue in Table 1 is \$/hour. Passenger surplus is calculated as  $\sum_{i=1}^M \sum_{j=1}^M \int_{c_{ij}}^{\infty} \lambda_{ij}^0 F_p(x) dx$ , while driver surplus is calculated as  $\int_0^q N_0 F_d(x) dx$ .

is also interesting to note that the platform assumes significantly higher tax burden than passengers and drivers under all congestion charge schemes.

	One-directional Cordon			Bi-directional Cordon			Trip-based Charge		
	Before charge	After charge	% change	Before charge	After charge	% change	Before charge	After charge	% change
passenger surplus	94,234	88,668	-5.91%	94,234	83,981	-10.88%	94,234	73,040	-22.49%
driver surplus	26,661	24,891	-6.64%	26,661	23,706	-11.08%	26,661	22,027	-17.38%
platform profit	64,749	57,693	-10.90%	64,749	53,150	-17.91%	64,749	45,510	-29.71%
tax revenue	0	5222	N.A.	0	8861	N.A.	0	22443	N.A.

Table 1: Distribution of tax burdens under distinct congestion charge schemes.

### 5.2.3. Sensitivity analysis

To understand how parameter values affect the aforementioned results, we conduct a sensitivity analysis by perturbing the key parameters in both directions by 30%. The following model parameters are selected for sensitivity study, including:  $\alpha, \epsilon, \sigma, \eta, N_0$  and  $\lambda_0$ .<sup>29</sup> We perturb these parameter values one by one while fixing other parameters at the nominal value, and solve the optimal spatial pricing problem under different values of the one-directional cordon price.<sup>30</sup> The total number of idle vehicles in the southwest corner of the city (including zip code zones 94122, 94116, 94132, 94112, 94124),  $N_S$ , and the passenger arrival rates for trips that start from the remote area and end in the remote area,  $\lambda_{22}$ , under distinct cordon prices are shown in Figure 50-61 of Appendix B. As the congestion charge is increased from \$0 to \$3, both  $N_S$  and  $\lambda_{22}$  increase for all values of the model parameters. It is clear that the insights derived in Section 5.2 always hold for all parameter values under the sensitivity test. Lastly, we point out that when the model parameters are perturbed by 30%, the total number of ride-sourcing trips at the optimal solution is perturbed by almost 50%. This indicates that the sensitivity study covers a large range of model parameters of practical interest, and the insights derived from the two-zone model are robust with respect to the variation of model parameters.

## 6. Conclusion

This paper evaluates the impact of congestion charges on the ride-sourcing market based on a network equilibrium model. The formulated model captures the intimate interactions among passenger waiting time, driver waiting time, passenger demand, driver supply, idle driver repositioning, traffic congestion, and network flow balance. The platform determines the location-differentiated price and driver payment, which induces a market equilibrium that in turn affects the platform profit. The overall problem is cast as a large-scale non-convex program. An algorithm is developed to approximately compute its optimal solution, and a tight upper bound is derived to characterize its performance. Based on the proposed model, we compared three forms of congestion charge: (a) a one-directional cordon-based charge that penalizes vehicles for entering the congestion area, (b) a bi-directional cordon-based charge that penalizes vehicles

<sup>29</sup>Since  $\lambda_0$  is a matrix, we perturb each entry of the matrices proportionately.

<sup>30</sup>We focus on the one-directional cordon price in the sensitivity study since the major insights are derived for this form of congestion charge.

for entering or exiting the congestion area, (c) a trip-based congestion charge on all ride-sourcing trips in the city. Through numerical study, we showed that the one-directional congestion charge not only reduces the ride-sourcing traffic in the congestion area, but also reduces the generalized travel cost outside the congestion area and benefits passengers in these underserved zones. We further show that compared to other congestion charges, the one-directional cordon charge is more effective in congestion mitigation, while the trip-based congestion charge is more effective in revenue-raising. The toll revenues collected from the congestion charges can be used to subsidize public transit, upgrade road infrastructure, or incentivize ridesourcing-transit integration to promote a more efficient multi-modal transportation system. Future study includes extending the framework to capture inter-zone matching, studying the network dynamics, and applying the analysis to other cities based on the ride-sourcing data.

## Acknowledgments

This research was supported by Hong Kong Research Grants Council under project HKUST26200420, the National Science Foundation EAGER award 1839843, and California Department of Transportation. We are very grateful to Joe Castiglione and Drew Cooper of San Francisco County Transportation Authority for guidance and data.

## References

- [1] NYCTLC. New York State’s Congestion Surcharge. New York City Taxi and Limousine Commission, 2019. <https://www1.nyc.gov/site/tlc/about/congestion-surcharge.page>.
- [2] New York State Assembly. Traffic mobility act A09633B. [https://assembly.state.ny.us/leg/?default\\_fld=&bn=9633&term=2015&Summary=Y&Memo=Y/](https://assembly.state.ny.us/leg/?default_fld=&bn=9633&term=2015&Summary=Y&Memo=Y/).
- [3] K. Pierog. Chicago approves traffic congestion tax on ride-hailing services. Reuters, 2019. <https://www.reuters.com/article/us-chicago-ridehailing-tax/chicago-approves-traffic-congestion-tax-on-ride-hailing-services-idUSKBN1Y02BV>.
- [4] Treasurer & Tax Collector. Traffic Congestion Mitigation Tax. <https://sftreasurer.org/business/taxes-fees/traffic-congestion-mitigation-tax-tcm#:~:text=The%20City%20imposes%20a%20Traffic,or%20private%20transit%20services%20vehicle>.
- [5] Tod Newcombe. Massachusetts Bets Big by Raising Ride-Sharing Surcharges. <https://www.governing.com/finance/Massachusetts-Bets-Big-by-Raising-Ride-Sharing-Surcharges.html/>.
- [6] J. Castiglione, D. Cooper, B. Sana, D. Tischler, T. Chang, G. D. Erhardt, S. Roy, M. Chen, and A. Mucci. TNCs & Congestion. Draft Report. San Francisco County Transportation Authority, 2018.
- [7] B. Schaller. Empty Seats, Full Streets. Fixing Manhattan’s Traffic Problem. Schaller Consulting, December 2017.
- [8] X. Qian, T. Lei, J. Xue, Z. Lei, and S. V. Ukkusuri. Impact of transportation network companies on urban congestion: Evidence from large-scale trajectory data. *Sustainable Cities and Society*, 55:102053, 2020.
- [9] M. Balding, T. Whinery, E. Leshner, and E. Womeldorff. Estimated TNC share of VMT in six US metropolitan regions. *Fehr & Peers*, 2019.

- [10] H. Yang and S.C. Wong. A network model of urban taxi services. *Transportation Research Part B: Methodological*, 32(4):235–246, 1998.
- [11] K. Wong, S. C. Wong, and H. Yang. Modeling urban taxi services in congested road networks with elastic demand. *Transportation Research Part B: Methodological*, 35(9):819–842, 2001.
- [12] H. Yang, S. C. Wong, and K. I. Wong. Demand–supply equilibrium of taxi services in a network under competition and regulation. *Transportation Research Part B: Methodological*, 36(9):799–819, 2002.
- [13] H. Yang, C. Leung, S. C. Wong, and M. Bell. Equilibria of bilateral taxi–customer searching and meeting on networks. *Transportation Research Part B: Methodological*, 44(8-9):1067–1083, 2010.
- [14] K. Wong, S. C. Wong, H. Yang, and J. Wu. Modeling urban taxi services with multiple user classes and vehicle modes. *Transportation Research Part B: Methodological*, 42(10):985–1007, 2008.
- [15] Z. Xu, Z. Chen, and Y. Yin. Equilibrium analysis of urban traffic networks with ride-sourcing services. *Available at SSRN 3422294*, 2019.
- [16] X. Ban, M. Dessouky, J. Pang, and R. Fan. A general equilibrium model for transportation systems with e-hailing services and flow congestion. *Transportation Research Part B: Methodological*, 129:273–304, 2019.
- [17] S. Ghili, V. Kumar, et al. Spatial distribution of supply and the role of market thickness: Theory and evidence from ride sharing. Technical report, Cowles Foundation for Research in Economics, Yale University, 2020.
- [18] K. Bimpikis, O. Candogan, and D. Saban. Spatial pricing in ride-sharing networks. *Operations Research*, 67(3):744–769, 2019.
- [19] L. Zha, Y. Yin, and Z. Xu. Geometric matching and spatial pricing in ride-sourcing markets. *Transportation Research Part C: Emerging Technologies*, 92:58–75, 2018.
- [20] X. Chen, C. Chen, and W. Xie. Optimal spatial pricing for an on-demand ride-sourcing service platform. *Available at SSRN 3464228*, 2019.
- [21] H. Guda and U. Subramanian. Your uber is arriving: Managing on-demand workers through surge pricing, forecast communication, and worker incentives. *Management Science*, 65(5):1995–2014, 2019.
- [22] H. Ma, F. Fang, and D. C. Parkes. Spatio-temporal pricing for ridesharing platforms. *arXiv preprint arXiv:1801.04015*, 2018.
- [23] F. Afifah and Z. Guo. Spatial pricing of ride-sourcing services in a congested transportation network. *arXiv preprint arXiv:2006.00164*, 2020.
- [24] F. He and Z. M. Shen. Modeling taxi services with smartphone-based e-hailing applications. *Transportation Research Part C: Emerging Technologies*, 58:93–106, 2015.
- [25] J. Qin, J. Porter, K. Poolla, and P. Varaiya. Piggyback on TNCs for electricity services: Spatial pricing and synergetic value. In *American Control Conference*. IEEE, 2020.
- [26] A. Pigou. *The economics of welfare*. MacMillan, London, 1920.
- [27] A. Walters. The theory and measurement of private and social cost of highway congestion. *Econometrica: Journal of the Econometric Society*, pages 676–699, 1961.
- [28] W. S. Vickrey. Pricing in urban and suburban transport. *The American Economic Review*, 53(2):452–465, 1963.

- [29] M. Beckmann. On optimal tolls for highways, tunnels, and bridges in vehicular traffic science. In *Proceedings of 3rd Symposium on the Theory of Traffic Flow*, 1965.
- [30] H. Yang and H. Huang. *Mathematical and economic theory of road pricing*. 2005.
- [31] C. R. Lindsey and E. T. Verhoef. Traffic congestion and congestion pricing. Technical report, Tinbergen Institute Discussion Paper, 2000.
- [32] A. D. May and D. S. Milne. Effects of alternative road pricing systems on network performance. *Transportation Research Part A: Policy and Practice*, 34(6):407–436, 2000.
- [33] X. Zhang and H. Yang. The optimal cordon-based network congestion pricing problem. *Transportation Research Part B: Methodological*, 38(6):517–537, 2004.
- [34] H. Yang, W. Xu, B. He, and Q. Meng. Road pricing for congestion control with unknown demand and cost functions. *Transportation Research Part C: Emerging Technologies*, 18(2):157–175, 2010.
- [35] A. Palma, M. Kilani, and R. Lindsey. Congestion pricing on a road network: A study using the dynamic equilibrium simulator metropolis. *Transportation Research Part A: Policy and Practice*, 39(7-9):588–611, 2005.
- [36] D. Wu, Y. Yin, and S. Lawphongpanich. Pareto-improving congestion pricing on multimodal transportation networks. *European Journal of Operational Research*, 210(3):660–669, 2011.
- [37] D. Wu, Y. Yin, S. Lawphongpanich, and H. Yang. Design of more equitable congestion pricing and tradable credit schemes for multimodal transportation networks. *Transportation Research Part B: Methodological*, 46(9):1273–1287, 2012.
- [38] M. D. Simoni, K. M. Kockelman, K. M. Gurumurthy, and J. Bischoff. Congestion pricing in a world of self-driving vehicles: An analysis of different strategies in alternative future scenarios. *Transportation Research Part C: Emerging Technologies*, 98:167–185, 2019.
- [39] N. Mehr and R. Horowitz. Pricing traffic networks with mixed vehicle autonomy. *arXiv preprint arXiv:1904.01226*, 2019.
- [40] M. Salazar, N. Lanzetti, F. Rossi, M. Schiffer, and M. Pavone. Intermodal autonomous mobility-on-demand. *IEEE Transactions on Intelligent Transportation Systems*, 2019.
- [41] S. Li, H. Tavafoghi, K. Poolla, and P. Varaiya. Regulating TNCs: Should Uber and Lyft set their own rules? *Transportation Research Part B: Methodological*, 2019.
- [42] S. Li, K. Poolla, and P. Varaiya. Impact of congestion charge and minimum wage on tncs: A case study for San Francisco. *arXiv preprint arXiv:2003.02550*, 2020.
- [43] H. Mohring, J. Schroeter, and P. Wiboonchutikula. The values of waiting time, travel time, and a seat on a bus. *The RAND Journal of Economics*, pages 40–56, 1987.
- [44] M. Nourinejad and M. Ramezani. Ride-sourcing modeling and pricing in non-equilibrium two-sided markets. *Transportation Research Part B: Methodological*, 132:340–357, 2020.
- [45] S. Banerjee, C. Riquelme, and R. Johari. Pricing in ride-share platforms: A queueing-theoretic approach. <https://ssrn.com/abstract=2568258>, 2015.
- [46] P. G. Harrison. Response time distributions in queueing network models. In *Performance Evaluation of Computer and Communication Systems*, pages 147–164. Springer, 1993.

- [47] A. Mas-Colell, M. D. Whinston, J. R. Green, et al. *Microeconomic theory*, volume 1. Oxford university press New York, 1995.
- [48] D. P. Bertsekas. *Nonlinear programming*. Athena Scientific Belmont, MA, 1998.
- [49] SFCTA. TNC pickup and dropoff data in San Francisco. <http://tncsandcongestion.sfcta.org/>, 2016.
- [50] R. Arnott. Taxi travel should be subsidized. *Journal of Urban Economics*, 40:316–333, 1996.
- [51] J. Castiglione, T. Chang, D. Cooper, J. Hobson, W. Logan, E. Young, B. Charlton, C. Wilson, A. Mislove, L. Chen, and Jiang S. TNCs today: a profile of San Francisco transportation network company activity. Final Report. San Francisco County Transportation Authority, 2017.
- [52] J. A. Parrott and M. Reich. An earnings standard for New York City’s app-based drivers: Economic analysis and policy assessment. The New School, Center for New York City Affairs , 2018.
- [53] Lyft. San Francisco Lyft rates. <https://estimatefares.com/rates/san-francisco>.
- [54] H. R. Varian. *Intermediate microeconomics with calculus: a modern approach*. WW Norton & Company, 2014.

## Appendix

### A: Sensitivity Analysis for Algorithm 1

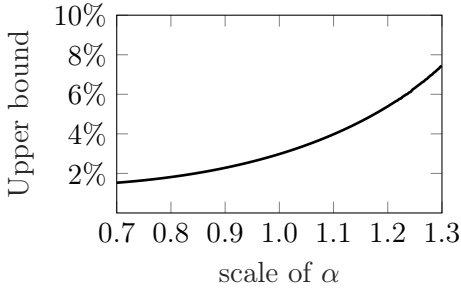


Figure 44: Upper bound on performance loss of Algorithm 1 by comparing (16) and (18) under distinct values of  $\alpha$ .

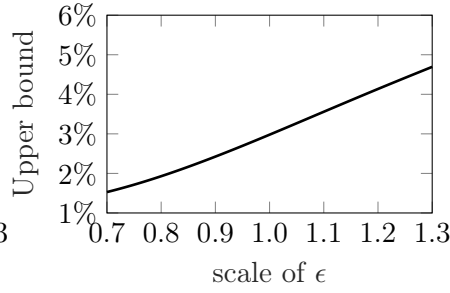


Figure 45: Upper bound on performance loss of Algorithm 1 by comparing (16) and (18) under distinct values of  $\epsilon$ .

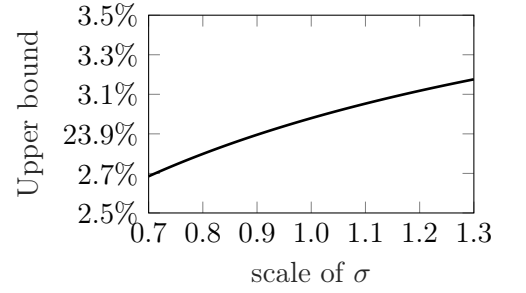


Figure 46: Upper bound on performance loss of Algorithm 1 by comparing (16) and (18) under distinct values of  $\sigma$ .

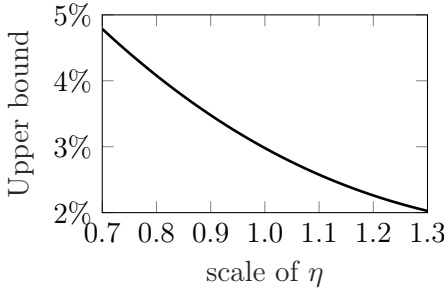


Figure 47: Upper bound on performance loss of Algorithm 1 by comparing (16) and (18) under distinct values of  $\eta$ .

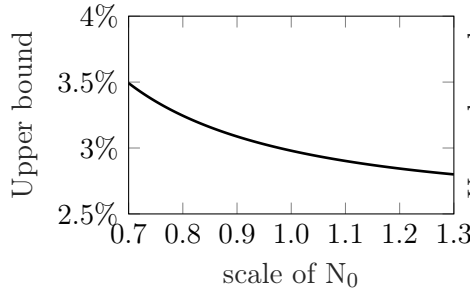


Figure 48: Upper bound on performance loss of Algorithm 1 by comparing (16) and (18) under distinct values of  $N_0$ .

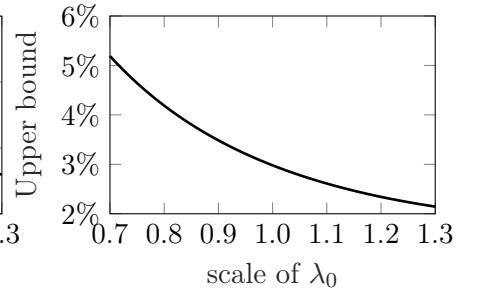


Figure 49: Upper bound on performance loss of Algorithm 1 by comparing (16) and (18) under distinct values of  $\lambda_0$ .

### B: Sensitivity Analysis for Impacts of Cordon Price in Two-Zone Model

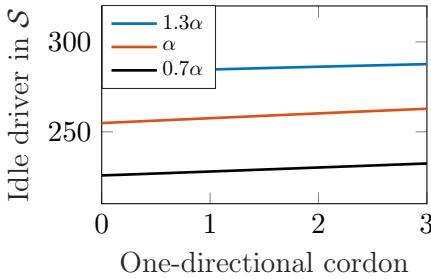


Figure 50: Number of idle drivers in southwest corner<sup>31</sup> under the one-directional cordon charge for distinct  $\alpha$

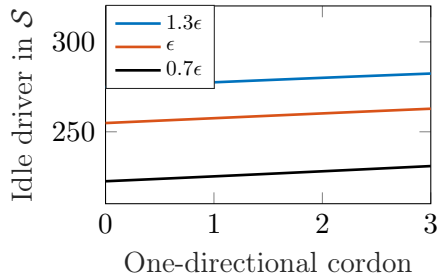


Figure 51: Number of idle drivers in southwest corner under the one-directional cordon charge for distinct  $\epsilon$ .

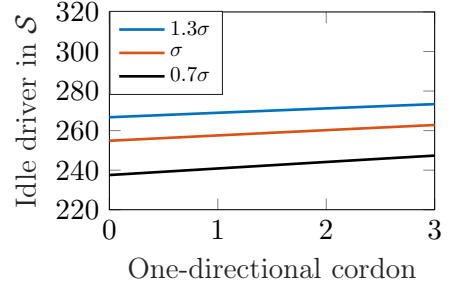


Figure 52: Number of idle drivers in southwest corner under the one-directional cordon charge for distinct  $\sigma$ .

<sup>31</sup>This includes zip code zones 94122, 94116, 94132, 94112, 94124.

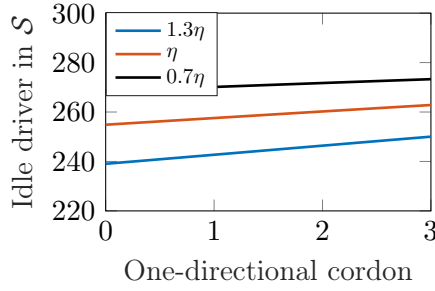


Figure 53: Number of idle drivers in southwest corner under the one-directional cordon charge for distinct  $\eta$ .

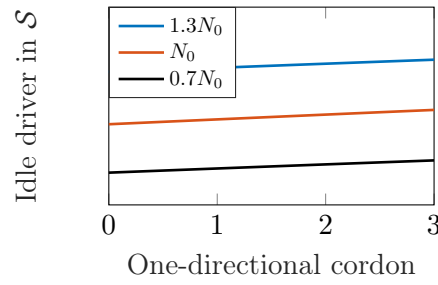


Figure 54: Number of idle drivers in southwest corner under the one-directional cordon charge for distinct  $N_0$ .

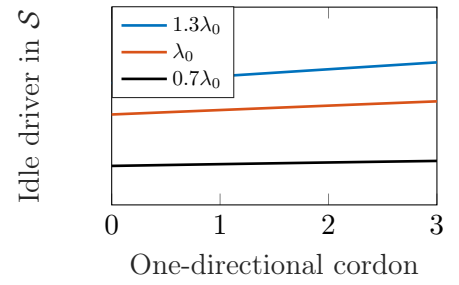


Figure 55: Number of idle drivers in southwest corner under the one-directional cordon charge for distinct  $\lambda_0$ .

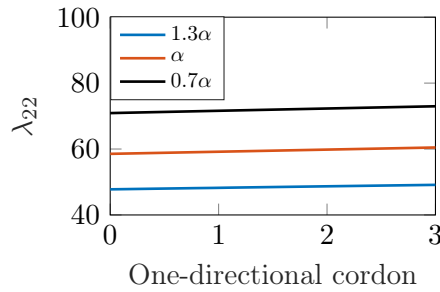


Figure 56:  $\lambda_{22}$  under the one-directional cordon charge for distinct  $\alpha$

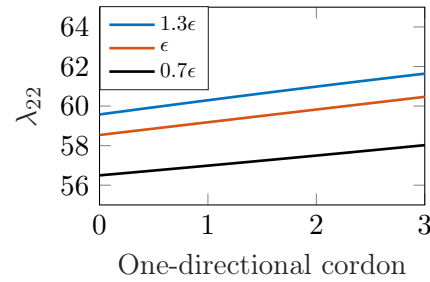


Figure 57:  $\lambda_{22}$  under the one-directional cordon charge for distinct  $\epsilon$ .

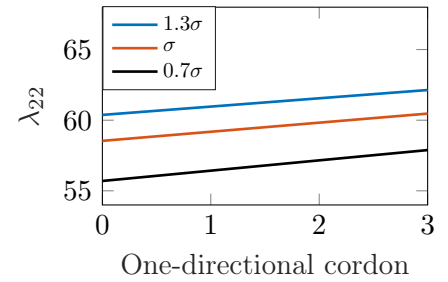


Figure 58:  $\lambda_{22}$  under the one-directional cordon charge for distinct  $\sigma$ .

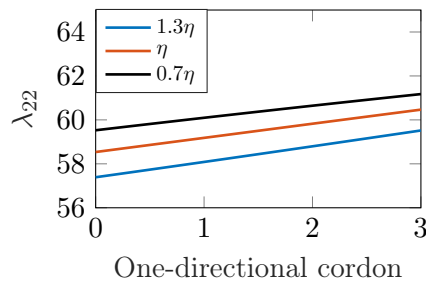


Figure 59:  $\lambda_{22}$  under the one-directional cordon charge for distinct  $\eta$ .

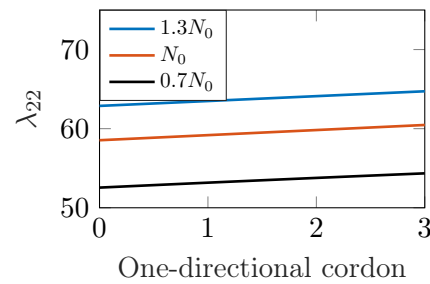


Figure 60:  $\lambda_{22}$  under the one-directional cordon charge for distinct  $N_0$ .

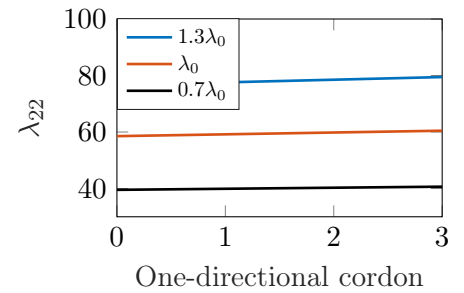


Figure 61:  $\lambda_{22}$  under the one-directional cordon charge for distinct  $\lambda_0$ .

### C: Results of the multi-zone simulation under congestion charges

Zip Code	Before one-directional cordon price					After one-directional cordon price				
	Idle vehicle	All vehicle <sup>32</sup>	Ride fare	Outflow to $\mathcal{C}$ <sup>33</sup> (/min)	Outflow to $\mathcal{R}$ (/min)	Idle vehicle	All vehicle	Ride fare	Outflow to $\mathcal{C}$ (/min)	Outflow to $\mathcal{R}$ (/min)
94104 <sup>34</sup>	72.9	200.0	\$2.00	8.14	1.70	66.6	180.8	\$2.09	7.35	1.44
94103	110.5	314.2	\$2.05	9.55	3.01	100.5	285.1	\$2.13	8.73	2.66
94109	114.0	337.6	\$2.08	8.77	4.28	100.4	299.6	\$2.16	7.89	3.75
94115	87.9	217.0	\$2.07	3.33	5.23	83.6	204.1	\$2.00	2.55	5.27
94118	115.4	237.0	\$2.09	4.63	6.89	108.1	227.4	\$2.01	3.99	6.98
94123	89.9	184.9	\$2.08	3.44	5.48	86.6	177.3	\$2.00	2.71	5.59
94108 <sup>35</sup>	114.5	279.5	\$2.04	10.30	3.41	105.7	253.6	\$2.14	9.37	2.97
94121	47.0	92.7	\$1.69	1.43	2.40	46.5	91.8	\$1.64	1.26	2.50
94102	117.9	308.9	\$2.06	8.08	3.86	106.7	278.0	\$2.17	7.29	3.37
94117	92.6	203.6	\$1.83	2.24	5.73	90.1	198.6	\$1.76	1.80	5.87
94122	78.5	182.6	\$1.82	1.79	6.65	79.3	184.3	\$1.77	1.58	6.86
94114	92.7	195.9	\$1.97	3.02	5.51	88.4	189.0	\$1.87	2.51	5.62
94107	88.8	217.8	\$1.87	6.96	3.24	81.8	198.3	\$1.94	6.36	2.91
94110	110.1	249.6	\$1.88	3.43	8.86	108.6	245.9	\$1.82	2.75	9.18
94131	69.6	138.6	\$1.68	1.49	2.99	68.3	139.1	\$1.56	1.40	3.11
94116	46.2	91.3	\$1.57	0.94	2.15	46.5	93.2	\$1.49	0.90	2.27
94124	45.5	81.4	\$1.51	0.88	1.77	45.5	81.3	\$1.44	0.76	1.86
94132	33.0	59.6	\$1.61	0.06	1.76	36.2	65.1	\$1.56	0.06	1.98
94112	51.6	95.6	\$1.65	0.11	3.11	55.3	101.9	\$1.60	0.10	3.37

Table 2: Ride-sourcing market before and after the one-directional cordon price is imposed.

<sup>30</sup>All vehicles include idle vehicles, occupied vehicles, and vehicles on the way to pick up a designated passenger.

<sup>31</sup>Outflow to  $\mathcal{C}$  denotes the passenger flow (per minute) with destinations in the congestion area  $\mathcal{C}$ .

<sup>32</sup>We use 94104 to represent the aggregated zone for zip code zones 94104, 94105, 94111.

<sup>33</sup>We use 94108 to represent the aggregated zone for zip code zones 94108 and 94133.

Zip Code	Before bi-directional cordon price					After bi-directional cordon price				
	Idle vehicle	All vehicle	Ride fare	Outflow to $\mathcal{C}$ (/min)	Outflow to $\mathcal{R}$ (/min)	Idle vehicle	All vehicle	Ride fare	Outflow to $\mathcal{C}$ (/min)	Outflow to $\mathcal{R}$ (/min)
94104	72.9	200.0	\$2.00	8.14	1.70	70.3	185.3	\$2.05	7.84	1.15
94103	110.5	314.2	\$2.05	9.55	3.01	105.3	285.6	\$2.06	9.34	2.17
94109	114.0	337.6	\$2.08	8.77	4.28	102.0	293.3	\$2.04	8.52	3.11
94115	87.9	217.0	\$2.07	3.33	5.23	72.1	179.9	\$2.09	2.12	4.57
94118	115.4	237.0	\$2.09	4.63	6.89	101.0	211.9	\$2.07	3.59	6.60
94123	89.9	184.9	\$2.08	3.44	5.48	78.4	160.8	\$2.09	2.32	5.05
94108	114.5	279.5	\$2.04	10.30	3.41	108.8	256.2	\$2.04	10.13	2.49
94121	47.0	92.7	\$1.69	1.43	2.40	43.2	84.8	\$1.68	1.11	2.28
94102	117.9	308.9	\$2.06	8.08	3.86	110.2	277.7	\$2.03	8.05	2.88
94117	92.6	203.6	\$1.83	2.24	5.73	84.4	183.2	\$1.85	1.51	5.34
94122	78.5	182.6	\$1.82	1.79	6.65	75.9	173.8	\$1.83	1.35	6.51
94114	92.7	195.9	\$1.97	3.02	5.51	83.4	175.8	\$1.97	2.19	5.20
94107	88.8	217.8	\$1.87	6.96	3.24	88.1	208.1	\$1.84	7.25	2.54
94110	110.1	249.6	\$1.88	3.43	8.86	99.8	226.4	\$1.88	2.41	8.43
94131	69.6	138.6	\$1.68	1.49	2.99	66.6	133.2	\$1.64	1.28	2.98
94116	46.2	91.3	\$1.57	0.94	2.15	45.1	88.9	\$1.54	0.81	2.16
94124	45.5	81.4	\$1.51	0.88	1.77	43.5	77.4	\$1.47	0.70	1.78
94132	33.0	59.6	\$1.61	0.06	1.76	35.0	62.1	\$1.60	0.05	1.85
94112	51.6	95.6	\$1.65	0.11	3.11	53.5	97.6	\$1.64	0.08	3.20

Table 3: Ride-sourcing market before and after the bi-directional cordon price is imposed.

Zip Code	Before trip-based charge					After trip-based charge				
	Idle vehicle	All vehicle	Ride fare	Outflow to $\mathcal{C}$ (/min)	Outflow to $\mathcal{R}$ (/min)	Idle vehicle	All vehicle	Ride fare	Outflow to $\mathcal{C}$ (/min)	Outflow to $\mathcal{R}$ (/min)
94104	72.9	200.0	\$2.00	8.14	1.70	58.0	155.8	\$1.90	5.47	1.26
94103	110.5	314.2	\$2.05	9.55	3.01	92.5	255.8	\$1.95	6.96	2.28
94109	114.0	337.6	\$2.08	8.77	4.28	96.1	275.6	\$1.98	6.45	3.22
94115	87.9	217.0	\$2.07	3.33	5.23	74.7	179.5	\$1.96	2.46	3.84
94118	115.4	237.0	\$2.09	4.63	6.89	102.8	208.8	\$1.98	4.04	5.71
94123	89.9	184.9	\$2.08	3.44	5.48	78.9	157.7	\$1.96	2.67	4.23
94108	114.5	279.5	\$2.04	10.30	3.41	102.3	235.3	\$1.92	7.99	2.83
94121	47.0	92.7	\$1.69	1.43	2.40	44.9	84.3	\$1.60	1.32	1.96
94102	117.9	308.9	\$2.06	8.08	3.86	104.4	260.2	\$1.93	6.27	3.05
94117	92.6	203.6	\$1.83	2.24	5.73	83.8	177.1	\$1.69	1.88	4.50
94122	78.5	182.6	\$1.82	1.79	6.65	74.0	166.1	\$1.72	1.67	5.65
94114	92.7	195.9	\$1.97	3.02	5.51	83.9	171.2	\$1.83	2.58	4.40
94107	88.8	217.8	\$1.87	6.96	3.24	80.4	186.2	\$1.77	5.53	2.65
94110	110.1	249.6	\$1.88	3.43	8.86	100.2	218.9	\$1.74	2.87	7.14
94131	69.6	138.6	\$1.68	1.49	2.99	65.3	127.7	\$1.54	1.41	2.57
94116	46.2	91.3	\$1.57	0.94	2.15	45.3	86.1	\$1.47	0.93	1.86
94124	45.5	81.4	\$1.51	0.88	1.77	45.1	78.1	\$1.38	0.85	1.61
94132	33.0	59.6	\$1.61	0.06	1.76	32.1	56.4	\$1.45	0.08	1.58
94112	51.6	95.6	\$1.65	0.11	3.11	49.3	89.0	\$1.48	0.12	2.77

Table 4: Ride-sourcing market before and after the trip-based charge is imposed.